Journal of Marine Science and Application (2019) 18:295–313
https://doi.org/10.1007/s11804-019-00104-7

RESEARCH ARTICLE

Influence of Support Conditions on the Hydroelastic Behaviour of Floating Thick Elastic Plate

K. M. Praveen[1] · D. Karmakar[1] · C. Guedes Soares[2]

Received: 6 May 2018 / Accepted: 12 November 2018 / Published online: 29 July 2019

Abstract
The hydroelastic response of very large floating structures (VLFS) under the action of ocean waves is analysed considering the small amplitude wave theory. The very large floating structure is modelled as a floating thick elastic plate based on Timoshenko-Mindlin plate theory, and the analysis for the hydroelastic response is performed considering different edge boundary conditions. The numerical study is performed to analyse the wave reflection and transmission characteristics of the floating plate under the influence of different support conditions using eigenfunction expansion method along with the orthogonal mode-coupling relation in the case of finite water depth. Further, the analysis is extended for shallow water depth, and the continuity of energy and mass flux is applied along the edges of the plate to obtain the solution for the problem. The hydroelastic behaviour in terms of reflection and transmission coefficients, plate deflection, strain, bending moment and shear force of the floating thick elastic plate with support conditions is analysed and compared for finite and shallow water depth. The study reveals an interesting aspect in the analysis of thick floating elastic plate with support condition due to the presence of the rotary inertia and transverse shear deformation. The present study will be helpful for the design and analysis of the VLFS in the case of finite and shallow water depth.

Keywords Timoshenko-Mindlin plate theory · Very large floating structure · Support condition · Rotary inertia · Transverse shear deformation

1 Introduction

The analysis and design of very large floating structures (VLFS) have increased significantly in the past few decades as compared with traditional offshore structures and land reclamation techniques. These structures have a lesser impact on the marine ecosystem, are rapid in installation and are immune to seismic activities as compared with other offshore structures. The VLFS are usually built in offshore regions, and the wavelength of ocean waves is in general too short as compared with the huge size of the structure to induce the rigid body motions. These structures are considered to be flexible as compared with other offshore structures, and hence, the study of hydroelastic behaviour is more important than the rigid body motions. These large floating structures are constructed for building infrastructures like floating airports, mobile offshore bases, floating cities, floating storage device and recreational parks. There has been a considerable study in the hydroelastic analysis of floating structures in the recent years, and many researchers performed a detailed study on the design and development of VLFS. The detailed review of the recent progress and future studies on the VLFS can be found in Kashiwagi (2000), Watanabe et al. (2004), Ohmatsu (2005), Chen et al. (2006) and Pardo et al. (2015). In addition, the application of VLFS is discussed and categorised the advantages and disadvantages of different types of VLFS in comparison with other types of

Article Highlights
- The hydroelastic response of VLFS under the action of ocean waves is analysed analytically.
- Timoshenko-Mindlin plate theory is considered which includes the effect of the rotary inertia and transverse shear deformation of the plate.
- The support conditions influences the hydroelastic behaviour of the floating thick elastic plate.

✉ D. Karmakar
dkarmakar@nitk.edu.in

[1] Department of Applied Mechanics and Hydraulics, National Institute of Technology Karnataka, Surathkal, Mangalore 575025, India

[2] Centre for Marine Technology and Ocean Engineering (CENTEC), Instituto Superior Técnico, Universidade de Lisboa, Av. Rovisco Pais, 1049 001 Lisbon, Portugal

floating structures. The study also includes various models, depths and proximity of the structures around the coast.

The hydroelastic analysis of a very large floating structure reported in the literatures is mostly based on the Euler-Bernoulli beam theory (Meylan and Squire 1994, 1996; Namba and Ohkusu 1999; Taylor and Ohkusu 2000; Khabakhpasheva and Korobkin 2002; Ohkusu and Namba 2004; Andrianov and Hermans 2003, 2006; Hermans 2003, 2004, 2007; Karmakar et al. 2009). The analysis using the Euler-Bernoulli beam theory neglects the effect of rotary inertia and shear deformation but the very large floating structures being huge in length and width also have a considerable depth. So, the study to include rotary inertia and shear deformation is very important for the hydroelastic response analysis. Mindlin (1951) introduced the theory to consider the effect of rotary inertia and shear deformation on elastic plates and the application of Timoshenko-Mindlin plate theory provides a better hydroelastic analysis of VLFS. Some of the significant studies considering the Timoshenko-Mindlin plate theory for the ocean wave interaction with ice floe/VLFS of infinite length are performed by Fox and Squire (1991), Balmforth and Craster (1999), Karmakar and Sahoo (2006), Tay and Wang (2012), Gao et al. (2013), Zhao et al. (2015) and Praveen et al. (2016, 2018). Most of the study on the hydroelastic behaviour of VLFS considers the structure to be freely floating based on free edge boundary condition. The wave interaction with large floating structures induces vertical and horizontal motions, and a mooring system is necessary to restrain the floating structure from wave-induced motion. In practical, the VLFSs are anchored to the seabed with a mooring system or supported at the edges by different edge conditions such as simply supported or fixed edge support.

In order to study the influence of edge support conditions, various researchers have attempted to consider different edge support conditions based on the requirement of the structure. Teng et al. (2001) used modified eigenfunction expansion method to analyse the reflection and transmission of ocean waves for semi-infinite thin elastic plate. The study was extended for the cases of simply supported and built-in edges, and it was demonstrated that the modified error function method satisfies well for the energy conservation relation at all three cases of edge conditions. Sahoo et al. (2001) developed orthogonal mode-coupling model based on eigenfunction expansion approach to study the scattering of waves due to a floating semi-infinite elastic plate in the case of finite water depth. The influence of different edge conditions was investigated for the case of free-free, simply supported and a built-in edge. The study summarized that the built-in edge condition induces the maximum wave reflection and the minimum wave transmission. The hydroelastic behaviour of a semi-infinite horizontal elastic plate floating on a homogenous fluid of finite depth is analysed by Xu and Lu (2009), and the study concluded that the plate thickness and the density of the plate do not influence the wave reflection and transmission characteristics. Kohout and Meylan (2009) studied the wave scattering by multiple floating elastic plates with spring connectors or hinges at the plate edges. The behaviour of the plate which is observed depends strongly on the boundary conditions at the plate edges. Xu and Lu (2011) developed an analytical method to analyse an arbitrary geometry of floating plate for the hydroelastic analysis based on thin plate theory. The analysis is performed considering vertical and angular eigenfunction methods to formulate different cases of edge boundary conditions. Gao et al. (2011) presented the hydroelastic response of pontoon-type, VLFS with a flexible line connection based on Mindlin plate theory. The modal expansion method is adopted in the frequency domain with combined BEM-FEM method. Karmakar and Guedes Soares (2012) analysed the wave scattering by a finite floating elastic plate connected with mooring lines at its corners in the presence of lateral pressure load. The hydroelastic behaviour of the floating elastic plate is investigated by analysing the effect of the stiffness of the mooring lines on the reflection and transmission characteristics of the gravity waves. Loukogeorgaki et al. (2014) implemented a 3D experimental and numerical investigation for the performance of a pontoon-type floating structure. The pontoon-type floating structure configuration is considered consisting of modules connected with hinge-type connectors and moored with chains. The study focused on the analysis of the wave characteristic effect on mooring line tension and hydroelastic response of the pontoon-type floating structure.

In the recent years, the hydroelastic performance of a floating structure is given more attention due to the increased design and analysis of multi-use combined platform for the development of infrastructure in the ocean environment. Wang et al. (2016) developed a finite element model to analyse the hydroelastic response of a horizontal elastic plate. The threshold values of the forward speed and compressive force for the beam are calculated for various lengths and different edge boundary conditions. The deflection in the middle points of the plate with three different boundary conditions is compared with available experimental and numerical results, and the study suggests that the deflection in the beam is affected largely due to the beam length and boundary conditions. The hydroelastic behaviour of an elastic floating plate connected to the sea bed using a time-domain approach was examined (Karperaki et al. 2016). The elastic plate is modelled based on the Euler-Bernoulli theory in shallow water depth, and the study mainly concentrates on the multiple elastic connectors joined by simple spring-dashpot systems along the structure. Guo et al. (2016) discussed the oblique wave scattering by a semi-infinite elastic plate with finite draft floating on the ocean with stepped topography. The effects of three different edge conditions are examined, and it was concluded that the change of the plate edge conditions has significant effects on

the plate deflection and moment. Loukogeorgaki et al. (2017) conducted 3D experiments to investigate the hydroelastic and the structural response of a pontoon-type modular floating breakwater moored with chains modules, under the action of perpendicular and oblique regular waves. The effect of the incident wave on the hydroelastic and structural response of the floating breakwater is analysed. Koley et al. (2018) performed the scattering of obliquely incident surface waves by a floating flexible porous plate in both the cases of finite and infinite water depths. The effects of three types of plate edge conditions, namely free-free, fixed and simply supported, are analysed, and the study suggested that the strain is lower in the case of a plate having free edges compared with that of fixed and simply supported edges.

In the present study, the wave interaction with VLFS is analysed based on the Timoshenko-Mindlin plate theory in both finite and shallow water depths for different edge support conditions. The hydroelastic behaviour of the floating elastic plate in finite water depth is compared for different edge boundary conditions. A mathematical model based on the eigenfunction expansion method along with mode-coupling relation (Karmakar et al. 2007) is used to analyse the wave interaction with VLFS. The generalized model is modified based on the Timoshenko-Mindlin plate theory to obtain the solution for the wave interaction with floating elastic plate in finite water depth. The numerical computation is performed to analyse the wave reflection and transmission characteristics and hydroelastic behaviour of the elastic plate under the action of a normally incident wave, and a comparative study of the free-free edge, simply supported edge and fixed edge condition is analysed in detail. The present analysis is restricted to normally incident waves on a floating plate of infinite extent in the transverse direction, and the extension to the case on an obliquely incident waves is presented in the Appendix A.

2 Mathematical Formulation

The wave interaction with the finite floating elastic plate with different edge support conditions is analysed based on the Timoshenko-Mindlin plate theory under the assumption of linearised wave theory. A two-dimensional coordinate system is considered for the wave-interaction with floating plate as shown in Fig.1. The wave is incident normally along the positive x-axis horizontally, and the y-axis is considered positive vertically downward. The thick elastic plate is considered to be floating at the free surface of the fluid ($I_2 \equiv -a < x < 0$, $y = 0$) and termed as plate-covered region 2. The open water surface divided into upstream open water domain ($I_1 \equiv 0 < x < \infty$, $0 < y < h$) termed as region 1 and downstream open water domain ($I_3 \equiv -\infty < x < -a$, $0 < y < h$) termed as region 3. The two edges of the floating thick elastic plate at $x = 0$ and $x = -a$ are considered to satisfy edge support boundary conditions.

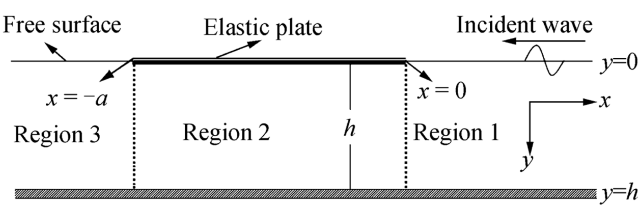

Fig. 1 Schematic diagram for floating elastic plate

Under the assumption of linearised wave theory, the velocity potential, Φ, satisfies Laplace's equation given by

$$\nabla^2 \Phi_j = 0 \ \text{ at } \ -\infty < x < \infty, 0 < y < h \tag{1}$$

The linearised kinematic boundary condition at the mean free surface is of the form

$$\zeta_{jt} = \Phi_{jy}, \quad \text{at} \quad y = 0 \tag{2}$$

The dynamic free surface boundary condition is given by

$$\rho \Phi_{jt} - \rho g \zeta_j = p_{\text{atm}} \quad \text{at} \quad y = 0 \tag{3}$$

where p_{atm} is the atmospheric pressure. The bottom boundary condition is given by

$$\Phi_{jy} = 0, \quad \text{at} \quad y = h \tag{4}$$

In the plate-covered region $j = 2$, it is assumed that the plate satisfies the Timoshenko-Mindlin theory (Fox and Squire 1991) which includes the effect of rotary inertia and transverse shear deformation of the form

$$\left(\partial_x^2 - \frac{\rho_p}{\mu G d}\partial_t^2\right)\left(EI\partial_x^2 - \frac{\rho_p d^3}{12}\partial_t^2\right)\zeta_j + \rho_p d \partial_t^2 \zeta_j = -\left(1 - \frac{EI}{\mu G d}\partial_x^2 + \frac{\rho_p d^2}{12\mu G}\partial_t^2\right)p \tag{5}$$

where d is the plate thickness, ρ_p is the plate density, $EI = Ed^3/12(1-\nu^2)$ is the plate rigidity, E is the Young modulus, ν is the Poisson ratio, $G = E/2(1+\mu)$ is the shear modulus of the plate, p is the pressure and μ is the transverse shear coefficient of the plate.

Assuming that the wave elevation and the plate deflection are simple harmonic motion in time with the frequency ω, the velocity potential $\Phi_j(x, y, t)$ and the surface deflection $\zeta_j(x, t)$ can be written as $\Phi_j(x, y, t) = \text{Re}\{\phi_j(x, y)\}e^{-i\omega t}$ and $\zeta_j(x, t) = \text{Re}\{\zeta_j(x)\}e^{-i\omega t}$ where Re denotes the real part. In the open water region, the linearised free surface boundary condition is given by

$$\phi_{jy}(x, y) - \kappa \phi_j(x, y) = 0, \quad \text{for } x > 0 \text{ and } x < -a \tag{6}$$

where $\kappa = \omega^2/g$. The plate-covered boundary condition in the region $j = 2$ is obtained by combining the linearised kinematic condition at the surface, Bernoulli's equation and Timoshenko-Mindlin equation as

$$\left\{\frac{EI}{(\rho g - m_s\omega^2)}\partial_x^4 + \left(\frac{m_s\omega^2 I}{(\rho g - m_s\omega^2)} - S\right)\partial_x^2 + \left(1 - \frac{m_s\omega^2 IS}{EI}\right)\right\}\phi_{jy}(x,y) \quad \text{for } -a < x < 0$$
$$+ \frac{\rho\omega^2}{(\rho g - m_s\omega^2)}\left\{1 - \frac{m_s\omega^2 IS}{EI} - S\partial_x^2\right\}\phi_j(x,y) = 0 \tag{7}$$

where ρ is the density of water, g is the acceleration due to gravity, $m_s = \rho_p d$ is the mass per unit area, ρ_p is the density of plate, d is the plate thickness, $I = d^2/12$ is the rotary inertia and $S = EI/\mu Gd$ is the shear deformation. The continuity of velocity and pressure at the interface $x = -a$ and $x = 0$ for $j = 1, 2; 0 < y < h$, is given by

$$\phi_{jx}(x,y) = \phi_{(j+1)x}(x,y) \text{ and } \phi_j(x,y) = \phi_{(j+1)}(x,y) \text{ at } x = -a \text{ and } x = 0, 0 < y < h \tag{8}$$

The far-field radiation condition is given by

$$\phi_j(x) = \begin{cases} \left(e^{-ik_{10}x} + R_0 e^{ik_{10}x}\right) f_{10}(y) & \text{as } x \to \infty \\ \left(T_0 e^{-ik_{30}x}\right) f_{30}(y) & \text{as } x \to -\infty \end{cases} \tag{9}$$

where R_0 and T_0 are the complex amplitudes of the reflected and transmitted waves. The eigenfunctions $f_{j0}(y)$'s for $j = 1, 3$ are of the form $f_{j0}(y) = \cosh k_{j0}(h - y)/\cosh k_{j0}h$ and k_{j0} for $j = 1, 3$ are the positive real roots which satisfy the dispersion relation in the case of finite water depth given by

$$k_{j0}\tanh k_{j0}h - \omega^2/g = 0 \tag{10}$$

3 Edge Support Condition of the Elastic Plate

The type of supports at the edge forms a boundary condition at the plate edges. In the wave interaction with floating elastic plate, different support conditions are considered in the study for the hydroelastic performance of the elastic plate under the action of ocean waves. The support conditions are based on the vertical shear forces along with the bending and twisting moments acting on the plate edges. These conditions represent the slope, deflection, bending moment and generalized shear force at the edges of the elastic plate. The consideration of the edge boundary condition in the hydroelastic analysis of large floating structures helps in the analysis and design of the VLFS. The major application of free-free edge boundary condition is in the study of the ocean wave interaction with the sea ice. The study mainly includes the wave attenuation due to the presence of sea ice and the breaking of the ice sheets due to incident ocean waves (Williams et al. 2013). However, most of the manmade large floating structures such as floating runways, floating oil storage base and offshore renewable energy plants need to be anchored at the edges by cables, ropes or piles to ensure safety and stability of structures. The floating oil storage base requires the structure to be stable under the action of ocean waves, which requires strong edge support to restrain the heave motion of the structure. Hence, the consideration of support conditions such as simply supported or fixed edge support condition becomes significant in the analysis. The floating elastic plate is considered to satisfy one of the following edge support conditions (Timoshenko and Krieger 1959; Rao 2007).

3.1 Freely Floating Elastic Plate

The freely floating elastic plate represents zero bending moment and zero shear force at the plate edge. In the case of finite water depth, the shear force and bending moment at the plate edge $x = 0, -a$ for $j = 2$ satisfy the relation given by

$$\partial_y^3\phi_j(x,y) = 0 \text{ and } \partial_{xy^3}^4\phi_j(x,y) = \wp\partial_{xy}^2\phi_j(x,y) \text{ for } x = 0, -a \text{ at } y = 0 \tag{11}$$

In the case of shallow water approximation, the zero shear force and zero bending moment at the plate edge $x = 0, -a$ satisfy the relation given by

$$\partial_x^4\phi_j(x) = 0 \text{ and } \partial_x^5\phi_j(x) = \wp\partial_x^3\phi_j(x) \text{ for } x = 0, -a \tag{12}$$

where $\wp = \left\{\frac{m\omega^2(S+I)}{EI}\right\}$.

3.2 Simply Supported Floating Elastic Plate

The simply supported edge condition represents the bending moment and deflection to vanish at the edges or at the supports for finite water depth. The plate edge is considered to be having zero deflection/displacement and zero bending moment at $x = 0, -a$ and $j = 2$ satisfying the relation

$$\partial_y\phi_j(x,y) = 0 \text{ and } \partial_y^3\phi_j(x,y) = 0 \text{ for } x = 0, -a \text{ at } y = 0 \tag{13}$$

In the case of shallow water approximation, the zero deflection/displacement and zero bending moment at the plate edge $x = 0, -a$ satisfy the relation

$$\partial_x^2\phi_j(x) = 0 \text{ and } \partial_x^4\phi_j(x) = 0 \text{ for } x = 0, -a \tag{14}$$

3.3 Fixed Edge Floating Elastic Plate

In the case of fixed edge condition, the deflection and slope vanish at the edge. So, for finite water depth, we consider zero slope and zero deflection/displacement at the plate edge $x = 0, -a$ and $j = 2$ which satisfy the relation

$$\partial_y \phi_j(x,y) = 0 \text{ and } \partial^2_{xy}\phi_j(x,y) = 0 \text{ for } x = 0, -a \text{ at } y = 0 \quad (15)$$

In the case of shallow water approximation, we consider zero slope and zero deflection/displacement at the plate edge $x = 0, -a$ which satisfy the relation

$$\partial^2_x \phi_j(x) = 0 \text{ and } \partial^3_x \phi_j(x) = 0 \text{ for } x = 0, -a \quad (16)$$

In the next section, the solution procedure for the wave interaction with the finite floating elastic plate is presented and discussed in detail.

4 Method of Solution

In this section, the scattering of waves due to the floating elastic plate is analysed based on the Timoshenko-Mindlin plate theory, and the solution procedure associated with the wave structure interaction is presented for both the cases of finite water depth and shallow water approximation.

4.1 Finite Water Depth

The boundary value problem for the scattering of the wave by a finite floating elastic plate with different edge boundary conditions is formulated in the case of finite water depth. The velocity potentials $\phi_j(x,y)$ for $j = 1, 2, 3$ satisfying governing Eq. (1) along with boundary conditions (4), (6), (7) and (9) are of the form

$$\begin{aligned}
\phi_1(x,y) &= \left(I_0 e^{-ik_{10}x} + R_0 e^{ik_{10}x}\right) f_{10}(y) + \sum_{n=1}^{\infty} R_n e^{-\kappa_{1n}x} f_{1n}(y) \quad \text{for } x > 0 \\
\phi_2(x,y) &= \sum_{n=0,I}^{II} \left(A_n e^{-ik_{2n}x} + B_n e^{ik_{2n}x}\right) f_{2n}(y) \\
&\quad + \sum_{n=1}^{\infty} \left(A_n e^{\kappa_{2n}x} + B_n e^{-\kappa_{2n}x}\right) f_{2n}(y) \quad \text{for} -a < x < 0 \\
\phi_3(x,y) &= T_0 e^{-ik_{30}x} f_{30}(y) + \sum_{n=1}^{\infty} T_n e^{\kappa_{3n}x} f_{3n}(y) \quad \text{for } x < -a
\end{aligned} \quad (17)$$

where R_n, $n = 0, 1, 2\ldots$, A_n, B_n, $n = 0$, I, II, 1, 2… and T_n, $n = 0, 1, 2\ldots$ are the unknown constants to be determined. The eigenfunctions $f_{jn}(y)$'s for $j = 2$ are given by

$$\begin{aligned}
f_{jn}(y) &= \frac{\cosh k_{jn}(h-y)}{\cosh k_{jn}h} \text{ for } n = 0, I, II \quad \text{and} \\
f_{jn}(y) &= \frac{\cos \kappa_{jn}(h-y)}{\cos \kappa_{jn}h} \text{ for } n = 1, 2, \ldots
\end{aligned} \quad (18a)$$

and the eigenfunctions $f_{jn}(y)$'s for $j = 1,\ 3$ are of the form

$$\begin{aligned}
f_{jn}(y) &= \frac{\cosh k_{jn}(h-y)}{\cosh k_{jn}h} \text{ for } n = 0 \text{ and } f_{jn}(y) \\
&= \frac{\cos \kappa_{jn}(h-y)}{\cos \kappa_{jn}h} \text{ for } n = 1, 2, \ldots
\end{aligned} \quad (18b)$$

where k_{jn} for $j = 1,\ 3$ and $n = 0$ are the eigenvalues which satisfy the dispersion relation in the open water region given by

$$k_{j0} \tanh k_{j0}h - \omega^2/g = 0 \quad (19)$$

with $k_{jn} = i\kappa_{jn}$ for $n = 1,\ 2\ldots$, and the dispersion relation has one real root k_{j0} and an infinite number of purely imaginary roots κ_{jn} for $n = 1,\ 2\ldots$ In the plate-covered region, the k_{jn} for $j = 2$ satisfies the dispersion relation given by

$$\left(\alpha_0 - \alpha_1 k^2_{jn} + \alpha_2 k^4_{jn}\right) k_{jn} \tanh k_{jn}h - \left(\beta_0 - \beta_1 k^2_{jn}\right) = 0 \quad (20)$$

where $\alpha_0 = \left\{1 - m_s\omega^2\left(\frac{IS}{EI}\right)\right\}$, $\alpha_1 = \left\{\frac{m_s\omega^2 I}{(\rho g - m_s\omega^2)} - S\right\}$, $\alpha_2 = \frac{EI}{(\rho g - m_s\omega^2)}$, $\beta_0 = \frac{\rho\omega^2}{(\rho g - m_s\omega^2)}\left(1 - m_s\omega^2\frac{IS}{EI}\right)$, $\beta_1 = -\frac{\rho\omega^2 S}{(\rho g - m_s\omega^2)}$ and $I = d^2/12$ are the rotary inertia, $EI = Ed^3/12(1-\nu^2)$ is the plate rigidity, $S = EI/\mu Gd$ is the shear deformation of the plate, $G = E/2(1+\nu)$ is the shear modulus of elastic material, $\mu = \frac{\pi^2}{12}$ is the transverse shear coefficient, E is Young's modulus, ν is Poisson's ratio and m_s is the mass of the plate. The dispersion relation as in Eq. (20) has two real roots k_{j0} and four complex roots k_{jn} for $n =$ I, II, III, IV of the form $\pm\alpha \pm i\beta$. In addition, there are infinite numbers of purely imaginary roots κ_{jn} for $n = 1,\ 2\ldots$.

In order to visualize the variation of the roots of the plate-covered dispersion relation, the contour plots are presented in Figs. 2(a)–(d) and 3 which demonstrate the existence of two real and four complex conjugate roots along with infinitely many imaginary roots for the plate-covered region. The occurrences of the infinitely many imaginary roots show the existence of evanescent modes (Manam et al. 2006). The roots of the dispersion relation are determined using the Newton-Raphson method and the contour plots help to identify the initial guess.

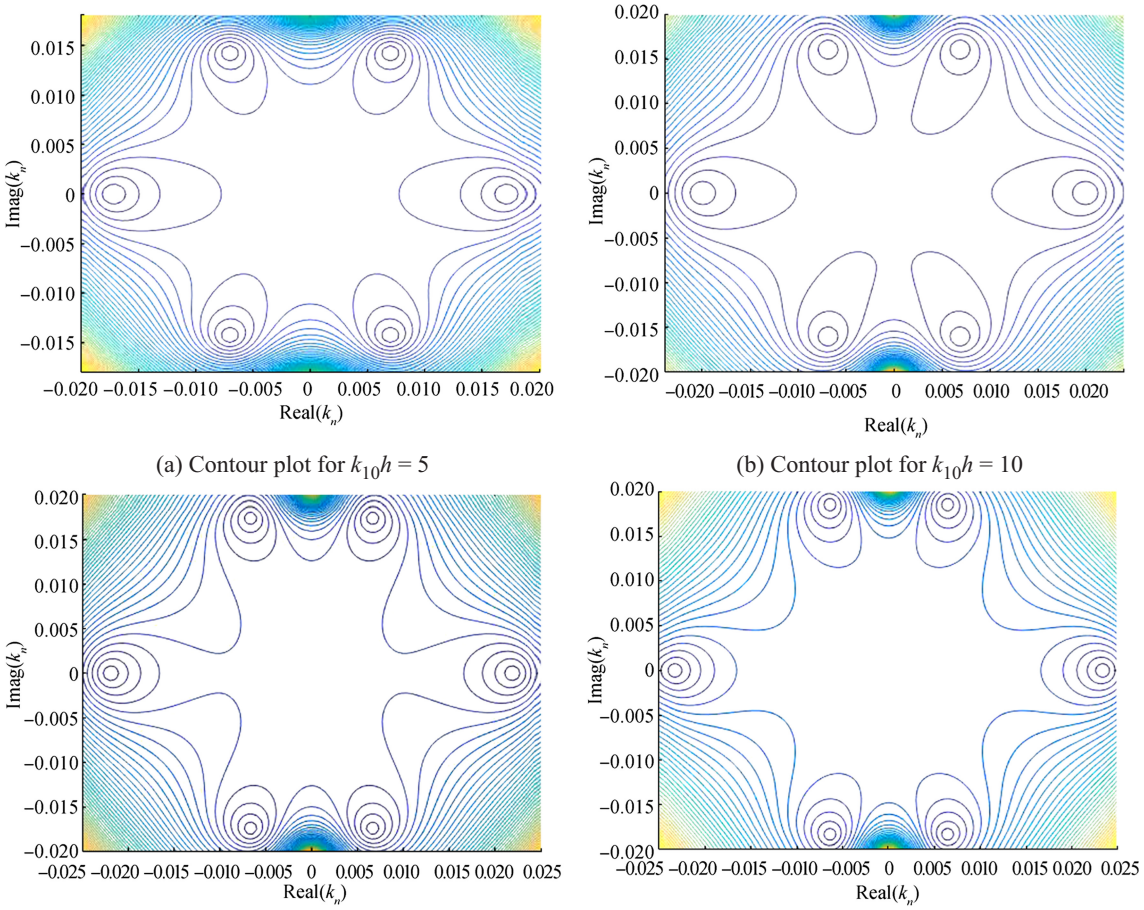

Fig. 2 Contour plot for the roots for the plate-covered dispersion relation considering $h/L = 0.15$, $E = 5$GPa and $d/L = 0.02$

It may be noted that the eigenfunctions $f_{jn}(y)$'s in the open water and plate-covered region satisfy the orthogonality relation as given by

$$\left\langle f_{jm}, f_{jn} \right\rangle_{j=1,3} = \begin{cases} 0 & \text{for } m \neq n, \\ C_n' & \text{for } m = n, \end{cases} \text{ and } \left\langle f_{jm}, f_{jn} \right\rangle_{j=2} = \begin{cases} 0 & \text{for } m \neq n \\ C_n'' & \text{for } m = n \end{cases} \tag{21}$$

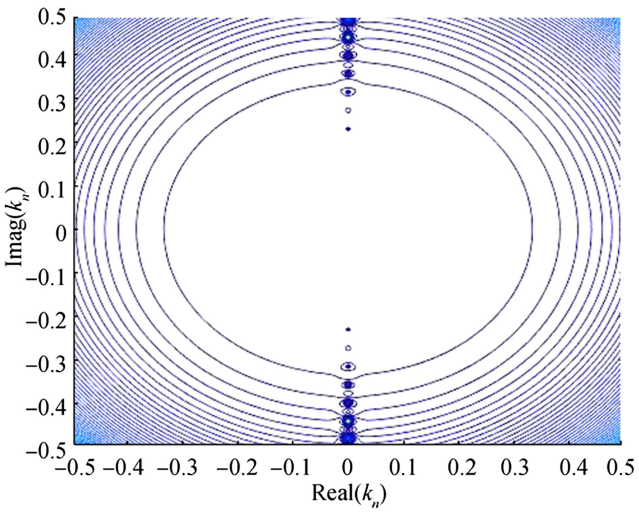

Fig. 3 Contour plot of infinite number of imaginary roots for the plate-covered dispersion relation considering $h/L = 0.15$, $E = 5$ GPa and $d/L = 0.02$ at $k_{10}h = 10$

with respect to the orthogonal mode-coupling relation defined by

$$\left\langle f_{jm}, f_{jn} \right\rangle_{j=1,3} = \int_0^h f_{jm}(y) f_{jn}(y) \mathrm{d}y \tag{22}$$

$$\begin{aligned} \left\langle f_{jm}, f_{jn} \right\rangle_{j=2} = {} & \int_0^h f_{jm}(y) f_{jn}(y) \mathrm{d}y - \frac{\alpha_1}{Q(k_{jn})} \left\{ f_{jm}'(0) f_{jn}'(0) \right\} \\ & + \frac{\alpha_2}{Q(k_{jn})} \left\{ f_{jm}'''(0) f_{jn}'(0) + f_{jm}'(0) f_{jn}'''(0) \right\} \\ & + \frac{\beta_1}{P(k_{jn})} f_{jm}(0) f_{jn}(0) \end{aligned} \tag{23}$$

where $C_n' = \frac{2k_{jn}h + \sinh 2k_{jn}h}{4k_{jn}\cosh^2 k_{jn}h}$ for $j = 1, 3$, $m = n = 0$

$$C_n'' = \frac{\left(\alpha_0 - \alpha_1 k_{jn}^2 + \alpha_2 k_{jn}^4\right) 2k_{jn}h + \left(\alpha_0 - 3\alpha_1 k_{jn}^2 + 5\alpha_2 k_{jn}^4\right) \sinh 2k_{jn}h + \left(4\beta_1 k_{jn} \cosh^2 k_{jn}h\right)}{\left(4k_{jn}\cosh^2 k_{jn}h\right)\left(\alpha_0 - \alpha_1 k_{jn}^2 + \alpha_2 k_{jn}^4\right)}$$
for $j = 2, m = n = 0, \mathrm{I}, \mathrm{II}$

with $P(k_{2n}) = \left(\alpha_0 - \alpha_1 k_{2n}^2 + \alpha_2 k_{2n}^4\right)$ and $Q(k_{2n}) = \left(\beta_0 - \beta_1 k_{2n}^2\right)$.

The constant terms $C_n^{'}$, $C_n^{''}$, $P(k_{jn})$ and $Q(k_{jn})$ for $n = 1, 2, \ldots$ are obtained by substituting $k_{jn} = \mathrm{i}\kappa_{jn}$ for $j = 1, 2, 3$. In order to determine the unknown coefficients, the mode-coupling relation is applied on the velocity potential along with the respective eigenfunction and the edge conditions to obtain the system of linear equation.

The mode-coupling relation as in Eq. (23) is applied on the velocity potential $\phi_2(x, y)$ at $x = 0, -a$ along with the eigenfunction $f_{2m}(y)$ to obtain the equations given by

$$\begin{aligned}\langle \phi_2(0,y), f_{2m}(y)\rangle = &\int_0^h \phi_2(0,y) f_{2m}(y)\mathrm{d}y - \frac{\alpha_1}{Q(k_{2n})}\left\{\phi_{2y}(0,y) f_{2m}^{'}(0)\right\} \\ &+ \frac{\alpha_2}{Q(k_{2n})}\left\{\phi_{2yyy}(0,0) f_{2m}^{'}(0) + \phi_{2y}(0,0) f_{2m}^{'''}(0)\right\} \\ &+ \frac{\beta_1}{P(k_{2n})}\phi_2(0,0) f_{2m}(0)\end{aligned} \tag{24a}$$

$$\begin{aligned}\langle \phi_2(-a,y), f_{2m}(y)\rangle = &\int_0^h \phi_2(-a,y) f_{2m}(y)\mathrm{d}y - \frac{\alpha_1}{Q(k_{2n})}\left\{\phi_{2y}(-a,y) f_{2m}^{'}(0)\right\} \\ &+ \frac{\alpha_2}{Q(k_{2n})}\left\{\phi_{2yyy}(-a,0) f_{2m}^{'}(0) + \phi_{2y}(-a,0) f_{2m}^{'''}(0)\right\} \\ &+ \frac{\beta_1}{P(k_{2n})}\phi_2(-a,0) f_{2m}(0)\end{aligned} \tag{24b}$$

for $m = 0$, I, II, 1, 2, ….

The mode-coupling relation as in Eq. (23) is applied on the velocity potential $\phi_{2x}(x, y)$ at $x = 0, -a$ along with the eigenfunction $f_{2m}(y)$ to obtain the equations given by

$$\begin{aligned}\langle \phi_{2x}(0,y), f_{2m}(y)\rangle = &\int_0^h \phi_{2x}(0,y) f_{2m}(y)\mathrm{d}y - \frac{\alpha_1}{Q(k_{2n})}\left\{\phi_{2xy}(0,y) f_{2m}^{'}(0)\right\} \\ &+ \frac{\alpha_2}{Q(k_{2n})}\left\{\phi_{2xyyy}(0,0) f_{2m}^{'}(0) + \phi_{2xy}(0,0) f_{2m}^{'''}(0)\right\} \\ &+ \frac{\beta_1}{P(k_{2n})}\phi_{2x}(0,0) f_{2m}(0)\end{aligned} \tag{25a}$$

$$\begin{aligned}\langle \phi_{2x}(-a,y), f_{2m}(y)\rangle = &\int_0^h \phi_{2x}(-a,y) f_{2m}(y)\mathrm{d}y - \frac{\alpha_1}{Q(k_{2n})}\left\{\phi_{2xy}(-a,y) f_{2m}^{'}(0)\right\} \\ &+ \frac{\alpha_2}{Q(k_{2n})}\left\{\phi_{2xyyy}(-a,0) f_{2m}^{'}(0) + \phi_{2xy}(-a,0) f_{2m}^{'''}(0)\right\} \\ &+ \frac{\beta_1}{P(k_{2n})}\phi_{2x}(-a,0) f_{2m}(0)\end{aligned} \tag{25b}$$

for $m = 0$, I, II, 1, 2, ….

The linear system of equation in Eqs. (24(a), (b)) and (25(a), (b)) is reformulated using the orthogonal property of the eigenfunction $f_{2m}(y)$ as in Eq. (21) along with continuity of pressure and velocity across the vertical interface $x = 0, -a$ and $0 < y < h$ as in Eq. (8). Further, the equations are simplified using the suitable edge boundary conditions to obtain a linear system of algebraic equations. The modified system of equation using the edge support condition is described in detail in the next subsection.

4.1.1 Free-Free Edge Support Condition

In the case of free-free edge condition, the bending moment and shear force terms vanish, and the system of equations is simplified as

$$\begin{aligned}&R_0\int_0^h f_{10}(y) f_{2m}(y)dy + \sum_{n=1}^{N+2} R_n \int_0^h f_{1n}(y) f_{2m}(y)\mathrm{d}y \\ &+ \left\{\sum_{n=0,I}^{II}(A_n + B_n) + \sum_{n=1}^{N}(A_n + B_n)\right\}\left[\frac{\alpha_2}{Q(k_{2n})} f_{2n}^{'}(0) f_{2m}^{'''}(0) - \frac{\alpha_1}{Q(k_{2n})} f_{2n}^{'}(0) f_{2m}^{'}(0)\right. \\ &\left. + \frac{\beta_1}{P(k_{2n})} f_{2n}(0) f_{2m}(0) - \delta_{mn}\langle f_{2n}, f_{2m}\rangle\right] = -I_0\int_0^h f_{10}(y) f_{2m}(y)\,\mathrm{d}y\end{aligned} \tag{26a}$$

$$\begin{aligned}&T_0 \mathrm{e}^{ik_{30}a}\int_0^h f_{30}(y) f_{2m}(y)\mathrm{d}y + \sum_{n=1}^{N+2} T_n \mathrm{e}^{-\kappa_{3n}a}\int_0^h f_{3n}(y) f_{2m}(y)\mathrm{d}y + \sum_{n=0,1,II}^{N}\left(A_n \mathrm{e}^{-ik_{2n}a} + B_n \mathrm{e}^{ik_{2n}a}\right) \\ &\left[\left\{\frac{\alpha_2}{Q(k_{2n})} f_{2n}^{'}(0) f_{2m}^{'''}(0) - \frac{\alpha_1}{Q(k_{2n})} f_{2n}^{'}(0) f_{2m}^{'}(0)\right\} + \frac{\beta_1}{P(k_{2n})} f_{2n}(0) f_{2m}(0) - \delta_{mn}\langle f_{2n}, f_{2m}\rangle\right] = 0\end{aligned} \tag{26b}$$

$$\begin{aligned}&ik_{10}R_0\int_0^h f_{10}(y) f_{2m}(y)\mathrm{d}y - \kappa_{1n}\sum_{n=1}^{N+2} R_n \int_0^h f_{1n}(y) f_{2m}(y)\mathrm{d}y + \left\{ik_{2n}\sum_{n=0,I}^{II}(A_n - B_n)\right. \\ &\left. -\kappa_{2n}\sum_{n=1}^{N}(A_n - B_n)\right\}\left[\frac{\alpha_2}{Q(k_{2n})}\left\{\wp f_{2n}^{'}(0) f_{2m}^{'}(0) + f_{2n}^{'}(0) f_{2m}^{'''}(0)\right\} - \frac{\alpha_1}{Q(k_{2n})} f_{2n}^{'}(0) f_{2m}^{'}(0)\right. \\ &\left. + \frac{\beta_1}{P(k_{2n})} f_{2n}(0) f_{2m}(0) - \delta_{mn}\langle f_{2n}, f_{2m}\rangle\right] = -ik_{10}I_0\int_0^h f_{10}(y) f_{2m}(y)\,\mathrm{d}y\end{aligned} \tag{26c}$$

$$\begin{aligned}&-ik_{30}T_0\mathrm{e}^{ik_{30}a}\int_0^h f_{30}(y) f_{2m}(y)\mathrm{d}y + \kappa_{3n}\sum_{n=1}^{N+2} T_n \mathrm{e}^{-\kappa_{3n}a}\int_0^h f_{3n}(y) f_{2m}(y)\mathrm{d}y \\ &+\left\{ik_{2n}\sum_{n=0,1}^{II}\left(A_n \mathrm{e}^{-ik_{2n}a} - B_n \mathrm{e}^{ik_{2n}a}\right) - \kappa_{2n}\sum_{n=1}^{N}\left(A_n \mathrm{e}^{\kappa_{2n}a} - B_n \mathrm{e}^{-\kappa_{2n}a}\right)\right\} \\ &\left[\frac{\alpha_2}{Q(k_{2n})}\left\{\wp f_{2n}^{'}(0) f_{2m}^{'}(0) + f_{2n}^{'}(0) f_{2m}^{'''}(0)\right\} - \frac{\alpha_1}{Q(k_{2n})} f_{2n}^{'}(0) f_{2m}^{'}(0)\right. \\ &\left. + \frac{\beta_1}{P(k_{2n})} f_{2n}(0) f_{2m}(0) - \delta_{mn}\langle f_{2n}, f_{2m}\rangle\right] = 0\end{aligned} \tag{26d}$$

for $m = 0$, I, II, 1, 2, ….

4.1.2 Simply Supported Edge Condition

In the case of simply supported edge condition, the bending moment and deflection terms vanish, and the system of equation is simplified as

$$\begin{aligned}&R_0\int_0^h f_{10}(y) f_{2m}(y)\mathrm{d}y + \sum_{n=1}^{N+2} R_n \int_0^h f_{1n}(y) f_{2m}(y)\mathrm{d}y + \left\{\sum_{n=0,1}^{II}(A_n + B_n) + \sum_{n=1}^{N}(A_n + B_n)\right\} \\ &\left[\frac{\beta_1}{P(k_{2n})} f_{2n}(0) f_{2m}(0) - \delta_{mn}\langle f_{2n}, f_{2m}\rangle\right] = -I_0\int_0^h f_{10}(y) f_{2m}(y)\,\mathrm{d}y\end{aligned} \tag{27a}$$

$$\begin{aligned}&T_0\mathrm{e}^{ik_{30}a}\int_0^h f_{30}(y) f_{2m}(y)\mathrm{d}y + \sum_{n=1}^{N+2} T_n \mathrm{e}^{-\kappa_{3n}a}\int_0^h f_{3n}(y) f_{2m}(y)\mathrm{d}y + \sum_{n=0,1,II}^{N}\left(A_n \mathrm{e}^{-ik_{2n}a} + B_n \mathrm{e}^{ik_{2n}a}\right) \\ &\left[\frac{\beta_1}{P(k_{2n})} f_{2n}(0) f_{2m}(0) - \delta_{mn}\langle f_{2n}, f_{2m}\rangle\right] = 0\end{aligned} \tag{27b}$$

$$ik_{10}R_0\int_0^h f_{10}(y)f_{2m}(y)\mathrm{d}y-\kappa_{1n}\sum_{n=1}^{N+2}R_n\int_0^h f_{1n}(y)f_{2m}(y)\mathrm{d}y+\left\{ik_{2n}\sum_{n=0,\mathrm{I}}^{\mathrm{II}}(A_n-B_n)+-\kappa_{2n}\sum_{n=1}^{N}(A_n-B_n)\right\}\left[\frac{\alpha_2}{Q(k_{2n})}\left\{f_{2n}^{'''}(0)f_{2m}^{'}(0)+f_{2n}^{'}(0)f_{2m}^{'''}(0)\right\}-\frac{\alpha_1}{Q(k_{2n})}f_{2n}^{'}(0)f_{2m}^{'}(0)+\frac{\beta_1}{P(k_{2n})}f_{2n}(0)f_{2m}(0)-\delta_{mn}\langle f_{2n},f_{2m}\rangle\right]=-ik_{10}I_0\int_0^h f_{10}(y)f_{2m}(y)\,\mathrm{d}y \tag{27c}$$

$$-ik_{30}T_0\mathrm{e}^{ik_{30}a}\int_0^h f_{30}(y)f_{2m}(y)\mathrm{d}y+\kappa_{3n}\sum_{n=1}^{N+2}T_n\mathrm{e}^{-\kappa_{3n}a}\int_0^h f_{3n}(y)f_{2m}(y)\mathrm{d}y+\left\{ik_{2n}\sum_{n=0,\mathrm{I}}^{\mathrm{II}}\left(A_n\mathrm{e}^{-ik_{2n}a}-B_n\mathrm{e}^{ik_{2n}a}\right)-\kappa_{2n}\sum_{n=1}^{N}\left(A_n\mathrm{e}^{\kappa_{2n}a}-B_n\mathrm{e}^{-\kappa_{2n}a}\right)\right\}\left[\frac{\alpha_2}{Q(k_{2n})}\left\{f_{2n}^{'''}(0)f_{2m}^{'}(0)+f_{2n}^{'}(0)f_{2m}^{'''}(0)\right\}-\frac{\alpha_1}{Q(k_{2n})}f_{2n}^{'}(0)f_{2m}^{'}(0)+\frac{\beta_1}{P(k_{2n})}f_{2n}(0)f_{2m}(0)-\delta_{mn}\langle f_{2n},f_{2m}\rangle\right]=0 \tag{27d}$$

for $m = 0$, I, II, 1, 2, ….

4.1.3 Fixed Edge/Built-in Edge Support Condition

In the case of fixed edge condition, the deflection and slope terms vanish, and the system of equation is simplified as

$$R_0\int_0^h f_{10}(y)f_{2m}(y)\mathrm{d}y+\sum_{n=1}^{N+2}R_n\int_0^h f_{1n}(y)f_{2m}(y)\mathrm{d}y+\left\{\sum_{n=0,\mathrm{I}}^{\mathrm{II}}(A_n+B_n)+\sum_{n=1}^{N}(A_n+B_n)\right\}\times\left[\frac{\alpha_2}{Q(k_{2n})}f_{2n}^{'''}(0)f_{2m}^{'}(0)+\frac{\beta_1}{P(k_{2n})}f_{2n}(0)f_{2m}(0)-\delta_{mn}\langle f_{2n},f_{2m}\rangle\right]=-I_0\int_0^h f_{10}(y)f_{2m}(y)\,\mathrm{d}y \tag{28a}$$

$$T_0\mathrm{e}^{ik_{30}a}\int_0^h f_{30}(y)f_{2m}(y)\mathrm{d}y+\sum_{n=1}^{N+2}T_n\mathrm{e}^{-\kappa_{3n}a}\int_0^h f_{3n}(y)f_{2m}(y)\mathrm{d}y+\sum_{n=0,\mathrm{I},\mathrm{II}}^{N}\left(A_n\mathrm{e}^{-ik_{2n}a}+B_n\mathrm{e}^{ik_{2n}a}\right)\times\left[\frac{\alpha_2}{Q(k_{2n})}f_{2n}^{'''}(0)f_{2m}^{'}(0)+\frac{\beta_1}{P(k_{2n})}f_{2n}(0)f_{2m}(0)-\delta_{mn}\langle f_{2n},f_{2m}\rangle\right]=0 \tag{28b}$$

$$ik_{10}R_0\int_0^h f_{10}(y)f_{2m}(y)\mathrm{d}y-\kappa_{1n}\sum_{n=1}^{N+2}R_n\int_0^h f_{1n}(y)f_{2m}(y)\mathrm{d}y+\left\{ik_{2n}\sum_{n=0,\mathrm{I}}^{\mathrm{II}}(A_n-B_n)-\kappa_{2n}\sum_{n=1}^{N}(A_n-B_n)\right\}\times\left[\frac{\alpha_2}{Q(k_{2n})}f_{2n}^{'''}(0)f_{2m}^{'}(0)+\frac{\beta_1}{P(k_{2n})}f_{2n}(0)f_{2m}(0)-\delta_{mn}\langle f_{2n},f_{2m}\rangle\right]=-ik_{10}I_0\int_0^h f_{10}(y)f_{2m}(y)\,\mathrm{d}y \tag{28c}$$

$$-ik_{30}T_0\mathrm{e}^{ik_{30}a}\int_0^h f_{30}(y)f_{2m}(y)\mathrm{d}y+\kappa_{3n}\sum_{n=1}^{N+2}T_n\mathrm{e}^{-\kappa_{3n}a}\int_0^h f_{3n}(y)f_{2m}(y)\mathrm{d}y+\left\{ik_{2n}\sum_{n=0,\mathrm{I}}^{\mathrm{II}}\left(A_n\mathrm{e}^{-ik_{2n}a}-B_n\mathrm{e}^{ik_{2n}a}\right)-\kappa_{2n}\sum_{n=1}^{N}\left(A_n\mathrm{e}^{\kappa_{2n}a}-B_n\mathrm{e}^{-\kappa_{2n}a}\right)\right\}\left[\frac{\alpha_2}{Q(k_{2n})}f_{2n}^{'''}(0)f_{2m}^{'}(0)+\frac{\beta_1}{P(k_{2n})}f_{2n}(0)f_{2m}(0)-\delta_{mn}\langle f_{2n},f_{2m}\rangle\right]=0 \tag{28d}$$

for $m = 0$, I, II, 1, 2, ….

Using the edge conditions, the linear equations as in Sections 4.1.1–4.1.3 for different edge conditions are truncated up to a finite number of N terms in order to solve the system of $(4N + 12)$ equations. The velocity potentials for each of the three regions as in Eq. (17) consist of $(4N + 12)$ unknown coefficients such as R_n, T_n, $n = 0$, 1, 2, ...N, $N + 1$, $N + 2$, A_n, B_n, $n = 0$, I, II, 1, 2, ..., N. On solving the system of the algebraic equation, the full solution is obtained in terms of the potential functions with the reflection and transmission coefficients which are obtained as

$$K_r = |R_0| \text{ and } K_t = \left|\frac{k_{30}\tanh k_{30}h}{k_{10}\tanh k_{10}h}T_0\right| \tag{29}$$

The reflection and transmission coefficients are observed to satisfy the energy balance relation $K_r^2 + K_t^2 = 1$.

4.2 Shallow Water Approximation

In the present section, the wave scattering due to finite floating thick elastic plate with different support conditions is analysed based on shallow water approximation. The geometry of the physical problem is considered the same as discussed in Section 2 but the wave motion is based on linearised long wave theory. Integrating the equation of continuity for fluids over the water depth, the relation between velocity potential and elevation for long waves is derived as

$$\zeta_{jt} = h\partial_x^2\Phi_j \quad \text{for} \quad j = 1, 2, 3 \tag{30}$$

The long wave equation of motion in the fluid domain for $j = 1, 3$ is given by

$$\Phi_{jt}-g\zeta_j = 0, \quad \text{for } x > 0 \text{ and } x < -a \tag{31}$$

Considering the wave elevation and deflection in the plate to be in simple harmonic in time with wave frequency ω, the velocity potential is expressed as $\Phi_j(x, t) = \mathrm{Re}\{\phi_j(x)\}\mathrm{e}^{-\mathrm{i}\omega t}$, and the elastic plate deflection is expressed as $\zeta_j(x, t) = \mathrm{Re}\{\zeta_j(x)\}\mathrm{e}^{-\mathrm{i}\omega t}$, where Re denotes the real part. Combining the long wave equation of continuity as in Eq. (30) and the long wave equation of motion in the fluid domain given by Eq. (31), the linearised long wave equation in the fluid domain is derived as

$$h\partial_x^2\phi_j - \kappa\phi_j = 0, \quad \text{for } x > 0 \quad \text{and} \quad x < -a \tag{32}$$

The long wave equation of motion in the plate-covered region is obtained by combining the equation of motion of the fluid and the Timoshenko-Mindlin plate equation given by

$$h\left\{\frac{EI}{(\rho g - m_s\omega^2)}\partial_x^4 + \left(\frac{m_s\omega^2 I}{(\rho g - m_s\omega^2)} - S\right)\partial_x^2 + \left(1 - \frac{m_s\omega^2 IS}{EI}\right)\right\}\partial_x^2\phi_2 + \frac{\rho\omega^2}{(\rho g - m_s\omega^2)}\left\{1 - \frac{m_s\omega^2 IS}{EI} - S\partial_x^2\right\}\phi_2 = 0, \quad \text{for } -a < x < 0 \tag{33}$$

where ρ is the density of water, m_s is the mass of the plate, ν is Poisson's ratio, $EI = Ed^3/12(1-\nu^2)$ is the flexural rigidity, E is Young's modulus, $G = E/2(1+\mu)$ is the shear modulus and μ is the transverse shear coefficient of the thick plate. The continuity of energy and mass flux at the interface $x = -a$ and $x = 0$ for $j = 1, 2$ is given by

$$\phi_{jx}(x) = \phi_{(j+1)x}(x) \text{ and } \phi_j(x) = \phi_{(j+1)}(x) \text{ at } x = -a \text{ and } x = 0 \tag{34}$$

Further, the floating elastic plate is considered to satisfy the edge support conditions as described in Section 3 for the case of shallow water depth. The far-field radiation condition in terms of velocity potential is given by

$$\phi_j(x) = \begin{cases} e^{-ik_{10}x} + R_0 e^{ik_{10}x} & \text{as } x \to \infty \\ T_0 e^{-ik_{30}x} & \text{as } x \to -\infty \end{cases} \tag{35}$$

where R_0 and T_0 are the complex coefficient of reflection and transmission and k_{j0} at $j = 1, 3$ are the roots of dispersion relation in shallow water

$$k_{j0}^2 - \left(\frac{\omega^2}{gh}\right) = 0 \tag{36}$$

In order to analyse the wave scattering by a floating elastic plate based on shallow water approximation, the fluid domain is divided into three subdomains as in Fig. 1. The velocity potentials $\phi_j(x)$ for $j = 1, 2, 3$ at the free surface and the plate-covered regions are of the form

$$\phi_j(x) = \begin{cases} \left(I_0 e^{-ik_{10}x} + R_0 e^{ik_{10}x}\right) & \text{for } x > 0 \\ A_0 e^{-ik_{20}x} + \overline{A}_0 e^{ik_{20}x} \sum_{n=\text{I,II}}^{\text{IV}} A_n e^{-ik_{2n}x} & \text{for } -a < x < 0 \\ T_0 e^{-ik_{30}x} & \text{for } x < -a \end{cases} \tag{37}$$

where R_0, T_0 and A_n, $n = 0$, I, .., IV and $\overline{A}_0$ are the unknown constants to be determined with k_{jn} at $j = 2$ and $n = 0$, I, II, III, IV are the eigenvalues that satisfy the dispersion relation

$$h\left[\frac{EI}{(\rho g - m_s\omega^2)}k_n^6 + \left(\frac{m_s\omega^2 I}{(\rho g - m_s\omega^2)} - S\right)k_n^4 + \left\{\left(1 - \frac{m_s\omega^2 IS}{EI}\right) - \frac{\rho\omega^2 S}{h(\rho g - m_s\omega^2)}\right\}k_n^2\right] - \frac{\rho\omega^2}{(\rho g - m_s\omega^2)}\left\{1 - \frac{m_s\omega^2 IS}{EI}\right\} = 0, \quad \text{for } -a < x < 0 \tag{38}$$

On application of the continuity equations as in Eq. (35) and edge boundary conditions as in Section 3 for the case of shallow water depth, a system of eight linear algebraic equations is obtained having the unknown constants R_0, T_0, A_0 and A_n, $n = 0$, I, …, IV. The unknown constants associated with the amplitude of the waves are determined by solving the system of algebraic equations. Once the unknowns R_0 and T_0 are obtained, the reflection and transmission coefficients are derived from the relation

$$K_r = |R_0| \quad \text{and} \quad K_t = \left|\left(\frac{k_{30}^2}{k_{10}^2}\right)T_0\right| \tag{39}$$

The reflection and transmission coefficients obtained for the shallow water approximation satisfy the energy balance relation $K_r^2 + K_t^2 = 1$.

5 Numerical Results and Discussions

The hydroelastic behaviour of the floating elastic plate under the action of the incident wave is analysed based on the Timoshenko-Mindlin theory in finite and shallow water depth. The study is performed to analyse the reflection coefficient K_r, transmission coefficient K_t, plate deflection ζ_j, bending moment $M(x)$, shear force $W(x)$ and strain on the plate ε for different support conditions. Three different cases of edge support condition, i.e. free-free edge, simply supported edge and fixed edge conditions, are considered and compared in the present study. The numerical computations are carried out for different water depths h/L and plate thickness d/L considering Young's modulus $E = 5$ GPa, $\rho_p/\rho_w = 0.9$, $\nu = 0.3$ and $g = 9.8\text{m}\cdot\text{s}^{-2}$. The numerical parameters such as plate length $L = 100$ m and non-dimensional wave number $k_{10}h = 5$ for finite water depth and $k_{10}h = 10$ for shallow water depth are considered to be fixed unless otherwise mentioned. The accuracy of the computed numerical results is checked with the energy relation which satisfies the energy balance relation $K_r^2 + K_t^2 = 1$.

The plate deflection versus the non-dimensional plate length is validated with the results obtained by Andrianov and Hermans (2006) as shown in Fig. 4 considering the plate length $L = 300$ m, plate thickness $d = 2$ m and wavelength $\lambda = 60$ m. The analysis of floating elastic plate is based on Kirchhoff thin plate theory by Andrianov and Hermans (2006), and the present method is based on the Timoshenko-Mindlin theory with negligible rotary inertia and transverse shear deformation in finite water depth. The results obtained using both the methods are observed to agree well considering the plate length $L = 300$ m. Further, it may be noted that with the increase in the plate length, the plate deflection increases which suggest that the hydroelastic behaviour is dominant

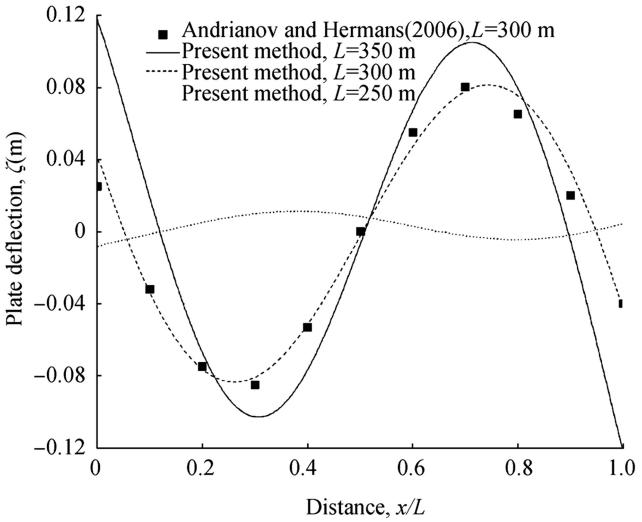

Fig. 4 Comparison of plate deflection with Andrianov and Hermans (2006) along the plate length considering rotary inertia $I = 0$ and shear deformation $S = 0$

than the rigid body motion with the increase in the length of the elastic plate.

5.1 Finite Water Depth

In this section, the wave scattering due to floating thick elastic plate in finite water depth is analysed considering different edge support conditions. The hydroelastic behaviour of the floating plate is studied by analysing the reflection and transmission coefficients, surface deflection, strain in the elastic plate, bending moment and shear force of the plate.

5.1.1 Reflection and Transmission Coefficient

The wave reflection and transmission coefficients for the floating elastic plate in relation (29) are having the same wave number in the incident and transmitted region. So the reflection and transmission coefficients reduces to

$$K_r = |R_0| \quad \text{and} \quad K_t = |T_0| \tag{40}$$

In Fig. 5(a), (b), the reflection and transmission coefficients are plotted versus non-dimensional wavenumber $k_{10}h$ for different support conditions considering $d/L = 0.02$ and $h/L = 0.15$. The zeros in the reflection coefficient at certain values of $k_{10}h$ indicate complete transmission of waves and may be termed as local minima. Initially for $0 < k_{10}h < 0.1$, the wave reflection is minimum, and the wave transmission is maximum for all the support conditions. The fixed edge support shows higher wave reflection as compared with the free-free edge and simply supported edge condition. The wave reflection coefficient approaches to one with the increase in $k_{10}h$ which suggests that for the wave with smaller wavelength, the wave reflection is higher. The forward shift in the zeros in the wave reflection and transmission coefficient is noted for different support conditions. The transmission coefficient approaching one indicates complete wave transmission for that particular $k_{10}h$. In the case of simply supported edge condition, the zeros in reflection coefficient or full wave transmission are observed for $5 < k_{10}h < 5.5$ and $16 < k_{10}h < 17$, whereas in the case of free-free edge condition, the full wave transmission is observed for $8 < k_{10}h < 9$. The study shows that the optimum values of wave reflection and transmission are higher for the simply supported edge condition.

5.1.2 Plate Deflection and Wave-Induced Strain

The plate deflection and wave-induced strain in the floating elastic plate are given by the relation

$$\zeta_j = \frac{i}{\omega}\phi_{jy} \quad \text{on} \quad y = 0, j = 2 \tag{41}$$

$$\varepsilon = \frac{d}{2}\partial_x^2\zeta_2 = \frac{id}{2\omega}\partial_{x^2y}^3\phi_2 \quad \text{at} \quad y = 0 \tag{42}$$

In Fig. 6(a), the surface deflection along the length of the plate for different support conditions is presented. The plate deflection is found to be least for simply supported edge and highest for free-free edge support condition. The lower value to plate deflection for simply supported edge condition and fixed edge condition as compared with free-free edge condition is due to the effect of restraints at the edge. Further, at the incident edge $x/L = 0$, the plate deflection is higher for fixed edge condition whereas at the transmitted edge $x/L = -1$, the plate deflection for the fixed edge is reduced and is observed higher for free-free edge condition. On the other hand, in Fig. 6b, the strain induced in the floating elastic plate due to the action of ocean waves is analysed for different support conditions. The wave-induced strain is found to be least for the simply supported edge and highest for fixed edge support condition. The strain along the floating elastic plate is higher for the free-free edge condition at the incident edge $x/L = 0$, whereas the strain in the transmitted edge $x/L = -1$ is higher for the fixed edge condition. Further, for the case of fixed edge support, it is observed that the wave-induced strain is reduced at the centre of the floating elastic plate due to higher rigidity at the edges of the structure.

5.1.3 Bending Moment and Shear Force

The bending moment and shear force of the floating elastic plate due to the interaction of wave are given by the relation

$$M(x) = EI\partial_y^3\phi_2 \quad \text{on} \quad y = 0 \tag{43}$$

$$W(x) = EI\left\{\partial_{xy^3}^4\phi_2 - \wp\partial_{xy}^2\phi_2\right\} \quad \text{on} \quad y = 0 \tag{44}$$

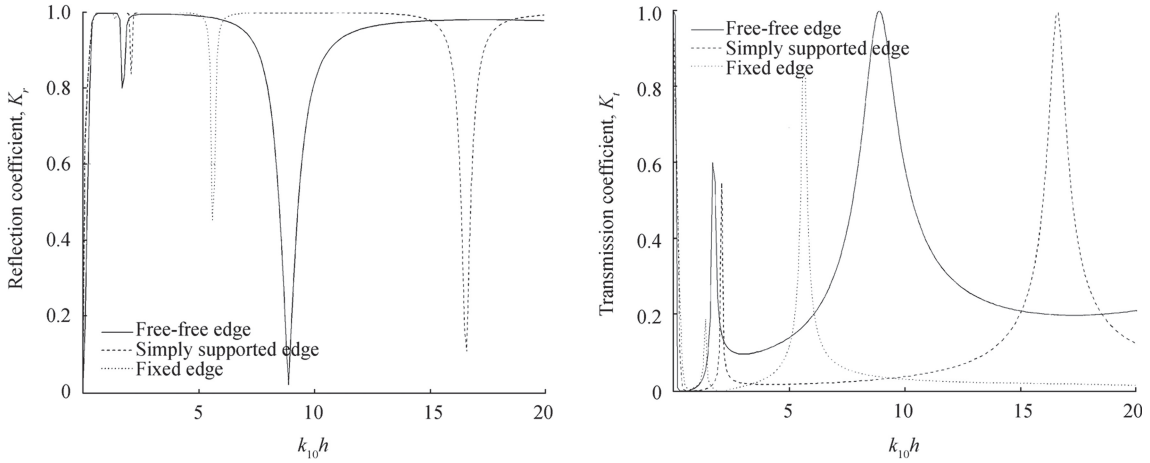

(a) Reflection coefficient (b) Transmission coefficient

Fig. 5 Wave reflection and transmission coefficients versus non-dimensional wavenumber $k_{10}h$ for different support conditions at $d/L = 0.02$ and $h/L = 0.15$

In Fig. 7(a), the bending moment resultants due to the wave interaction with the floating elastic plate are plotted along the plate length for different support conditions. The bending moment resultant is observed to be least for the floating structure with a simply supported edge and highest for free-free edge support condition. On the other hand, the bending moment is observed to increase at the centre of the structure for the case of free-free edge support which may be due to the change in the phase of the incoming and outgoing waves propagating below the floating elastic plate. The shear force resultants (Fig. 7(b)) due to the wave interaction with the floating elastic plate are plotted along the plate length for different support conditions. The shear force resultant is observed to be least for floating structure with a simply supported edge and highest for the free-free edge support condition as observed similar in the case of bending moment along the plate length. The shear force and bending moment for the simply supported edge and fixed edge condition are minimum at the incident edge $x/L = 0$ and at the transmitted edge $x/L = -1$. Further, at the centre of the plate, the shear force is higher for the free-free edge condition as compared with the simply supported and fixed edge conditions.

5.2 Comparison of Thin and Thick Elastic Plate

The comparison of the thin and thick elastic plate based on the Timoshenko-Mindlin plate theory and Kirchhoff's plate theory for the simply supported edge condition and fixed edge condition is presented. The detailed comparison of thin and thick plate is performed on analysing the hydroelastic characteristics of the floating elastic plate.

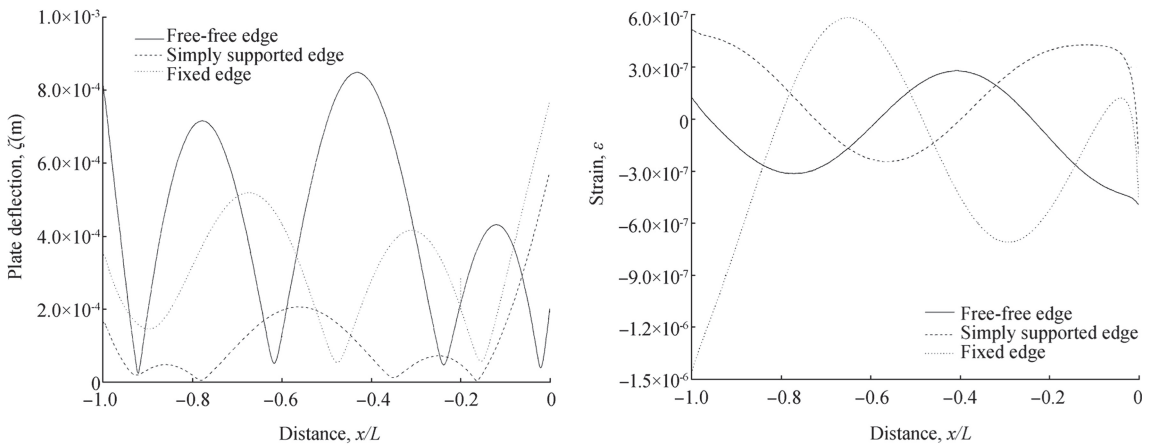

(a) Plate deflection (b) Wave induced strain of floating plate

Fig. 6 Plate deflection and wave-induced strain along the plate length x/L for different edge support conditions at $k_{10}h = 5$, $d/L = 0.02$ and $h/L = 0.15$

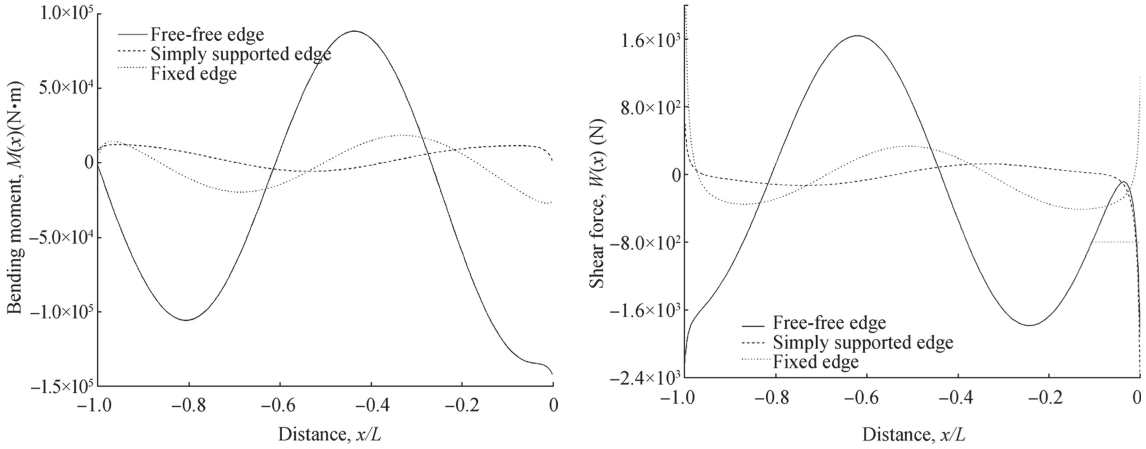

(a) Bending moment of floating plate (b) Shear force of floating plate

Fig. 7 Bending moment and shear force resultants along the plate length x/L for different edge support conditions at $k_{10}h = 5$, $d/L = 0.02$ and $h/L = 0.15$

5.2.1 Simply Supported Edge Condition

The wave reflection and transmission coefficients (Fig. 8(a), (b)) based on the thin plate theory is compared with thick plate theory varying non-dimensional wave number in the case of simply supported edge condition. The wave reflection and transmission characteristics for both the plate theories are the same for $0 < k_{10}h < 2.5$, but with the increase in the non-dimensional wave number, the deviation in the K_r and K_t is noted. The wave transmission is observed more for the thin plate theory for higher values of non-dimensional wave number. This suggests that for lower wavelength, the wave transmission is more in the case of the thin plate theory. The Timoshenko-Mindlin plate theory shows higher resistance to wave transformation, whereas the complete transmission peaks are observed to be similar for both the theories. The comparison using both plate theories suggests that the presence of rotary inertia and shear deformation is significant in the wave transformation and hydroelastic behaviour of the floating elastic plate.

In Fig. 9(a)–(d), the plate deflection, wave-induced strain, bending moment and shear force of a floating elastic plate are compared based on Timoshenko-Mindlin's plate theory and Kirchhoff's plate theory for the simply supported edge condition. The variation in the plate deflection (Fig. 9(a)) using both the plate theories is minimal but the deflection is higher at the plate centre and at the incident edge $x/L = 0$ of the plate. A significant variation in the strain in the floating elastic plate (Fig. 9(b)) using both Kirchhoff's plate theory and Timoshenko-Mindlin plate theory is noted. The strain in the floating elastic plate is higher for the Timoshenko-Mindlin plate theory. The bending moment and shear force (Fig. 9(c), (d)) are higher for Kirchhoff's plate theory as compared with the Timoshenko-Mindlin plate theory. Thus, the study shows

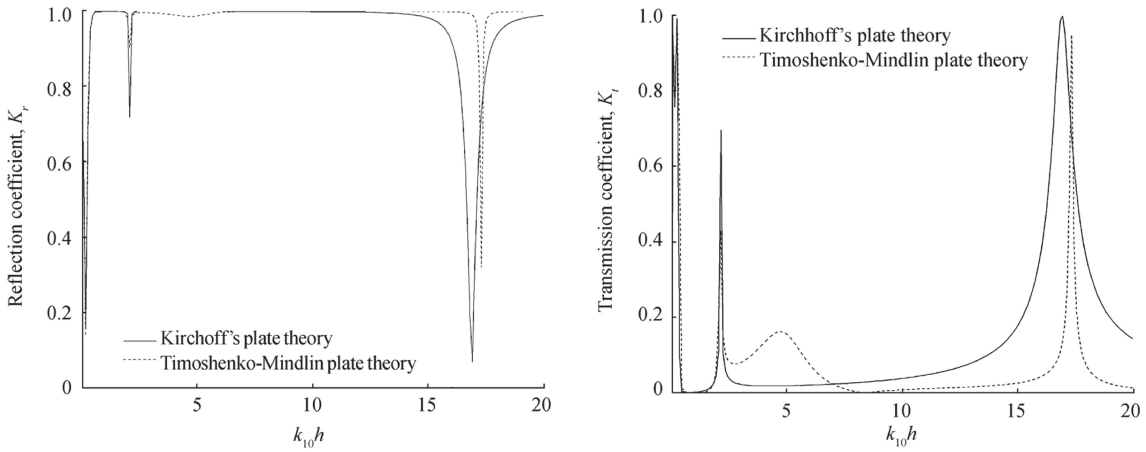

(a) Reflection coefficient (b) Transmission coefficient

Fig. 8 Wave reflection and transmission coefficient versus non-dimensional wavenumber $k_{10}h$ considering $E = 5$ GPa and $h/L = 0.15$, $d/L = 0.02$

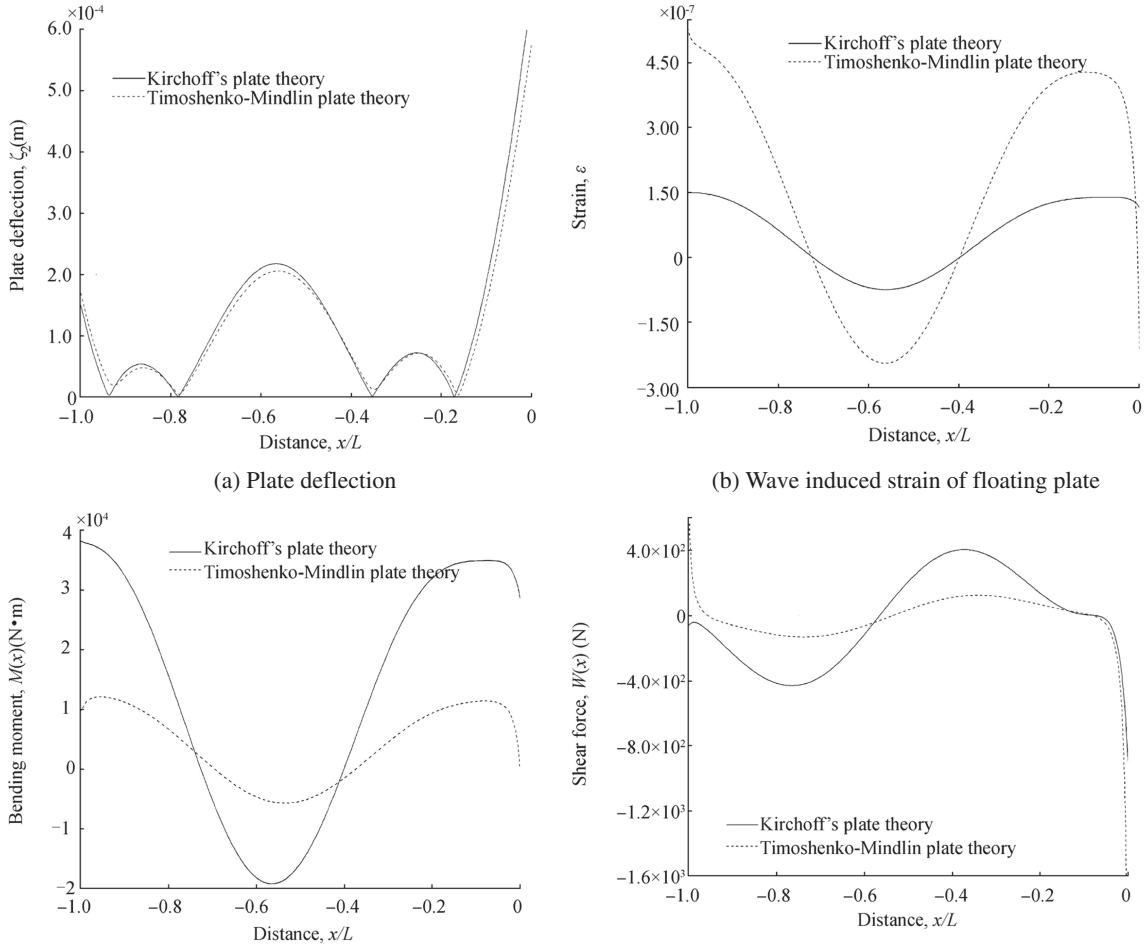

Fig. 9 Plate deflection, wave-induced strain, bending moment and shear force along the plate length considering $k_{10}h = 5$, $E = 5$ GPa and $h/L = 0.15$, $d/L = 0.02$

that due to the presence of rotary inertia and shear deformation, a significant reduction in bending moment and shear force with a slight reduction in plate deflection and increase in wave-induced strain is obtained as compared with Kirchhoff's thin plate theory.

5.2.2 Fixed Edge Support Condition

The wave reflection and transmission coefficients based on Kirchhoff's thin plate theory is compared with the Timoshenko-Mindlin plate theory versus the non-dimensional wave number for the fixe edge condition in Fig.10(a), (b). The variation in the K_r and K_t is significant for $2.5 < k_{10}h < 7.5$, and with the increase in the non-dimensional wave number, the variation is minimal. The wave reflection and transmission characteristics using the Timoshenko-Mindlin plate theory are higher whereas the complete transmission of waves is observed to be the same within $5 < k_{10}h < 5.5$ for both the plate theories. The variation of K_r and K_t using both the theories suggests that the presence of rotary inertia and shear deformation plays a significant role in the wave transformation and hydroelastic behaviour of fixed edge supported floating elastic plate.

The hydroelastic behaviour in terms of plate deflection, wave-induced strain, bending moment and shear force of a floating elastic plate with fixed edge support is compared based on Timoshenko-Mindlin's plate theory and Kirchhoff's plate theory in Fig. 11(a)–(d). The variation in plate deflection (Fig. 11(a)) is significant as compared using both Timoshenko-Mindlin's plate theory and Kirchhoff's plate theory.

The plate deflection near the incident edge $x/L = 0$ is higher for Kirchhoff's plate theory whereas at the central plate section, the plate deflection using the Timoshenko-Mindlin plate theory is slightly more as compared to Kirchhoff's plate theory. The strain (Fig. 10(b)) in the floating elastic plate is higher for the Timoshenko-Mindlin plate theory, and the reduction in the bending moment and shear force (Fig. 11(a), (b)) is observed for the Timoshenko-Mindlin plate theory. Thus, the presence of rotary inertia and shear deformation shows

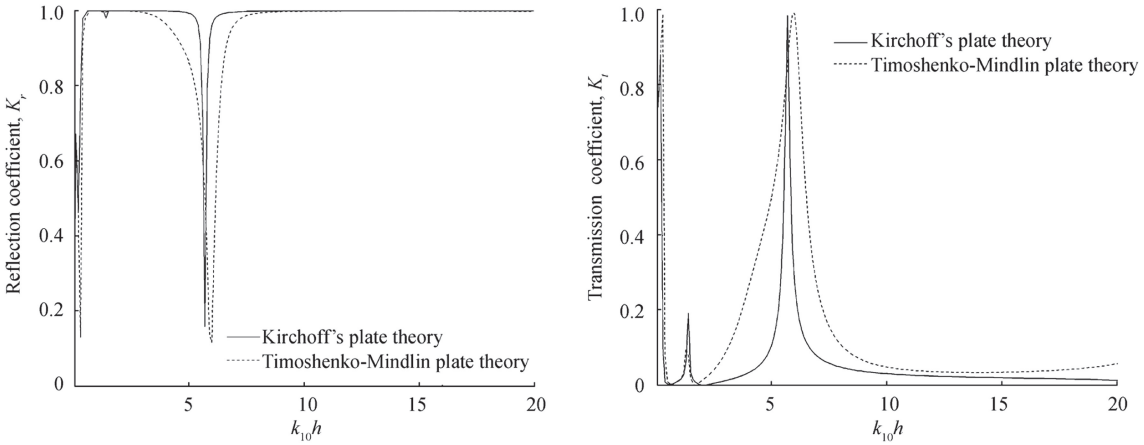

(a) Reflection coefficient (b) Transmission coefficient

Fig. 10 Wave reflection and transmission coefficients versus non-dimensional wavenumber $k_{10}h$ considering $E = 5$ GPa and $h/L = 0.15$, $d/L = 0.02$

reduction in the plate deflection, wave-induced strain, bending moment and shear force at the incident edge of the floating plate, whereas an increase in hydroelastic behaviour is observed at the transmitted edge.

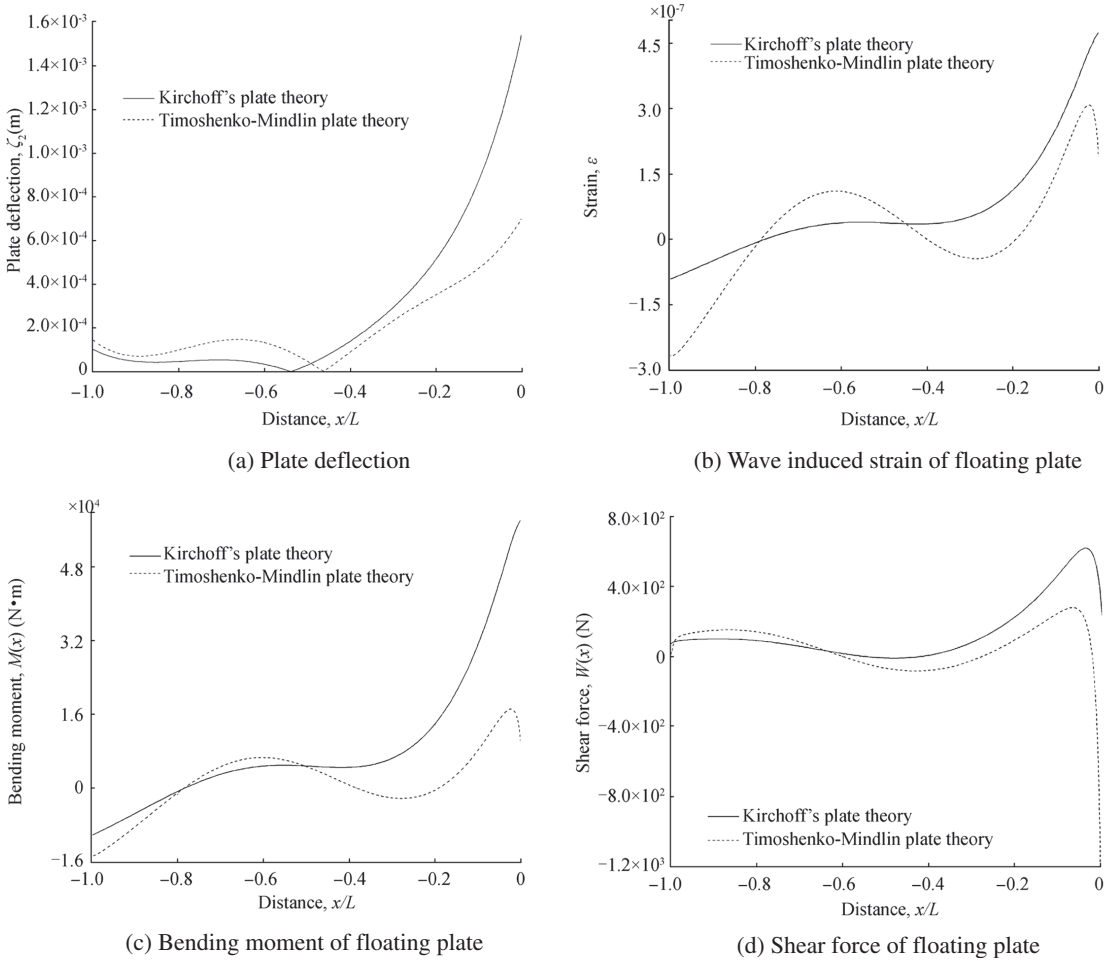

(a) Plate deflection (b) Wave induced strain of floating plate

(c) Bending moment of floating plate (d) Shear force of floating plate

Fig. 11 Plate deflection, wave-induced strain, bending moment and shear force along the plate length considering $k_{10}h = 3$, $E = 5$ GPa and $h/L = 0.15$, $d/L = 0.02$

5.3 Shallow Water Approximation

In this section, the wave interaction with a floating elastic plate is analysed based on shallow water approximation. The hydroelastic behaviour of the floating elastic plate in shallow water depth is analysed and compared with the different cases of edge support conditions.

5.3.1 Reflection and Transmission Coefficient

The reflection and transmission coefficients for the floating elastic plate based on shallow water approximation are the same as described in Eq. (40). In Fig. 12(a), (b), the reflection and transmission coefficients versus the non-dimensional wave number are plotted for different cases of edge support conditions. It is observed that the zeros in the wave reflection are least for the free-free edge support condition and higher for the fixed edge support condition. At very low values of non-dimensional wave number, the variation in reflection and transmission coefficients is observed to be more as compared with higher values of $k_{10}h$. Further, higher transmission of waves is observed at very low frequencies for the free-free edge support condition due to zero restraints at the edges. The simply supported edge is observed to transmit a higher number of waves as compared with fixed support edge but lesser than the free-free support condition due to the constraint in deflection at the edges.

5.3.2 Plate Deflection and Wave-Induced Strain

The plate deflection and wave-induced strain of the elastic plate in shallow water depth are given by the relation

$$\zeta_j = \frac{\mathrm{i}h}{\omega}\partial_x^2\phi_j \quad \text{for } j = 2 \tag{45}$$

$$\varepsilon = \frac{d}{2}\partial_x^2\zeta_2 = \frac{\mathrm{i}dh}{2\omega}\partial_x^4\phi_2 \tag{46}$$

The plate deflection along the length of the plate at different edge support conditions is presented in Fig. 13(a). The plate deflection is observed to be zero at the edges of the plate for the case of simply supported and fixed edge support conditions, which is due to restraints at the edges. The plate deflection is observed to be higher at the edges of the plate for the free-free edge boundary condition due to zero restraints at the edges. Due to the zero deflection at the plate edge for the simply supported edge and fixed edge conditions, the deflection is observed to be lesser for the simply supported edge and fixed edge conditions as compared with the free-free edge support.

In Fig.13(b), the strain induced in the plate due the action of ocean waves is plotted for different support edge conditions. It is observed that the wave-induced strain is highest at the plate edges for the fixed edge support condition and zero for the cases of the free-free edge and simply supported edge conditions which is mainly due to restraints in the plate for the corresponding edge conditions. A lower strain is observed for the free-free edge and simply supported edge due non-zero slope condition. An increase in wave-induced strain is observed at the centre of the structure for the case of the fixed edge condition due to zero slope condition.

5.3.3 Bending Moment and Shear Force

The bending moment and shear force of the floating elastic plates are given by

$$M(x) = EI\partial_x^4\phi_2 \tag{47}$$

$$W(x) = EI\left\{\partial_x^5\phi_2 - \wp\partial_x^3\phi_2\right\} \tag{48}$$

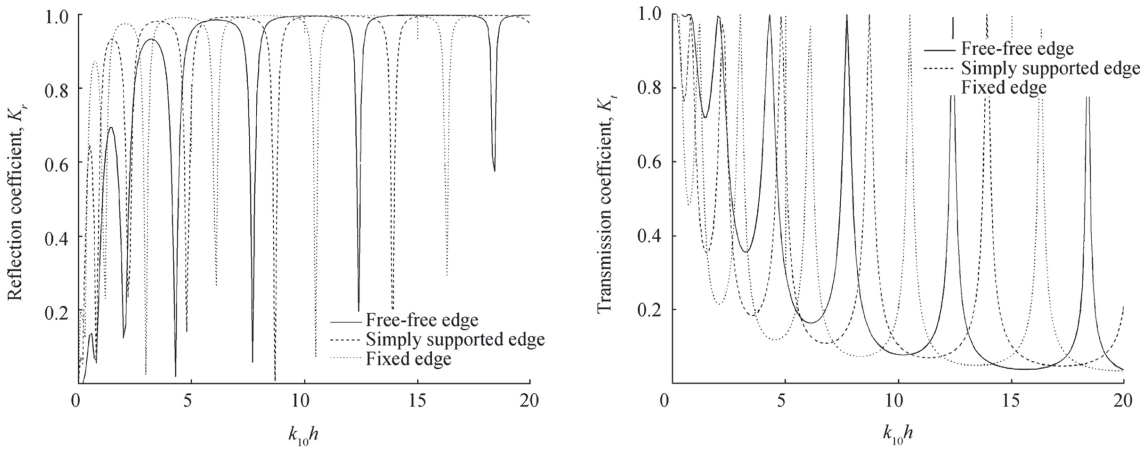

(a) Reflection coefficient (b) Transmission coefficient

Fig. 12 Wave reflection and transmission coefficients versus non-dimensional wavenumber $k_{10}h$ for different support conditions at $d/L = 0.02$ and $h/L = 0.10$

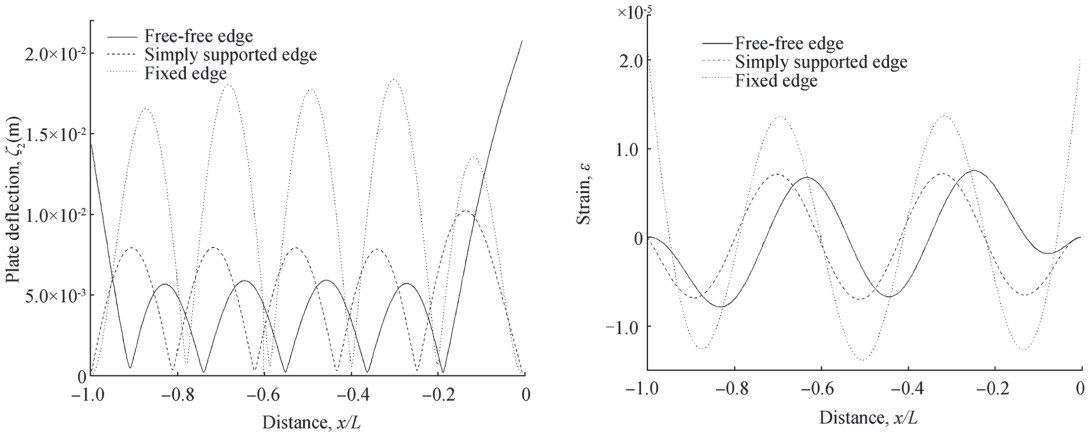

(a) Plate deflection (b) Wave induced strain of floating plate

Fig. 13 Plate deflection and wave-induced strain along the plate length x/L for different edge support conditions at $k_{10}h = 10$, $d/L = 0.02$ and $h/L = 0.10$

In Fig. 14(a), the bending moment on the plate due to incident waves is plotted along the length of the plate for different edge support conditions. At the edges of the plate, the bending moment is observed to be zero for the case of a free-free edge and simply supported edge due to zero moment condition. On the other hand, a maximum bending moment is observed at the edges and at the centre of the structure due to the edge restraints in the case of the fixed edge support condition. The shear force on the plate due to incident waves is plotted along the length of the plate in Fig. 14(b) for different edge support conditions. At the plate edges, zero shear force is observed for the case of a free-free edge condition but for the case of the fixed edge support, a maximum shear force is observed at the edges and zero at the centre of the structure due to edge constraints.

6 Conclusion

The influence of edge support conditions on the hydroelastic behaviour of floating elastic plate based on the Timoshenko-Mindlin plate theory is analysed. The study of normally incident wave on floating elastic plate is performed for finite and shallow water depths. The numerical study is performed based on the eigenfunction expansion method. The wave reflection and transmission coefficients are computed and observed to satisfy the energy balance relation for both the cases of water depths. The hydroelastic characteristics of floating elastic plate are compared for different support conditions. In addition, a brief comparison of the numerical results for the simply supported edge condition and fixed edge condition for both Kirchhoff's plate theory and Timoshenko-Mindlin plate theory is discussed in detail. The results demonstrating the effects of wave directionality on the application of the present model

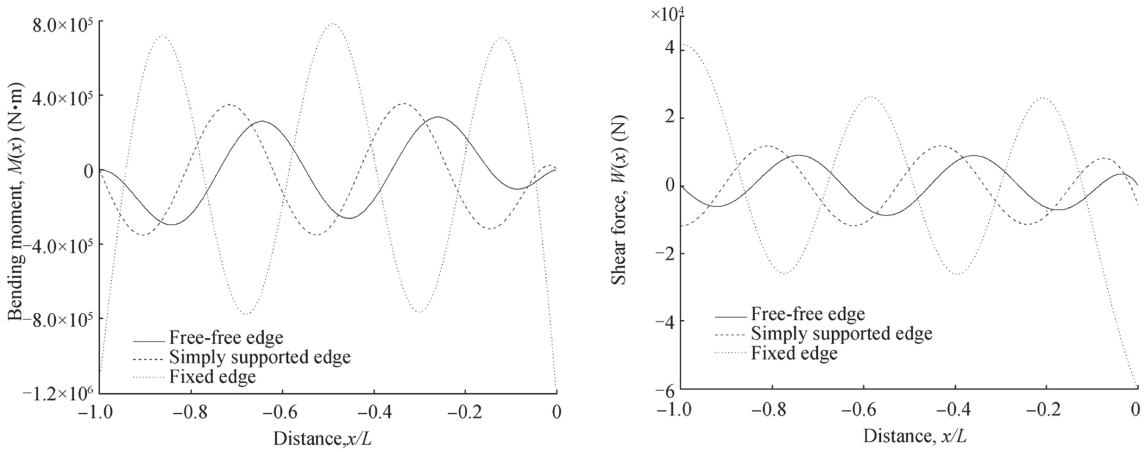

(a) Bending moment of floating plate (b) Shear force of floating plate

Fig. 14 Bending moment and shear force resultants along the plate length x/L for different edge support conditions at $k_{10}h = 10$, $d/L = 0.02$ and $h/L = 0.10$

will be presented in the future work. The following conclusions drawn from the present study are as follows:

- The high variations in reflection and transmission behaviour are observed for higher values of non-dimensional wave numbers for different support conditions in the case of finite and shallow water depths.
- The free-free edge support condition shows higher transmission of waves whereas lower wave transmission for the fixed edge support is observed at finite and shallow water depths.
- The hydroelastic behaviour is found to be higher for the free-free edge support conditions and least for the fixed edge due to restraints from the boundary conditions in the case of finite water depth. On the other hand, the bending moment and shear force resultants are found to be highest for the fixed edge support and least for the simply supported edge condition in the case of shallow water depth.
- The bending moment is observed to increase at the centre of the structure for the case of the free-free edge support at finite water depth which may be due to the change in the phase of the incoming and outgoing waves propagating below the floating elastic plate.
- The comparison of the floating elastic plate for different edge conditions using both Kirchhoff's plate theory and Timoshenko-Mindlin's plate theory suggests that the presence of rotary inertia and shear deformation is significant in the hydroelastic behaviour of the floating elastic plate.
- At shallow water depth, the plate deflection is observed to be zero for the case of the simply supported and fixed edge support conditions. Further, wave-induced strain is found to be zero for the free-free edge and simply supported edge conditions.
- The bending moment and shear force resultants are zero for the free-free edge and simply supported edge due to the restraints at the edges in shallow water depth.

Funding The authors are thankful to NITK Surathkal and MHRD for providing financial and necessary support to perform the research work. The authors also acknowledge the Science and Engineering Research Board (SERB), Department of Science & Technology (DST), Government of India, for supporting financially under the Young Scientist research grant No. YSS/2014/000812.

Appendix A: Oblique Wave Interaction with Floating Thick Plate

The oblique wave interaction with the finite floating elastic plate is analysed based on the Timoshenko-Mindlin plate theory for different edge support conditions. In Fig. A1, the wave is obliquely incident along the $x-z$ plane horizontally and the y–axis is considered vertically downward positive. The floating plate is considered to extend infinitely along the z–axis and floating along $-a<x<0$. The elastic plate is assumed to be at finite water depth, and a monochromatic wave is obliquely incident at an angle θ. The edges of the plate at $x=0$ and $x=-a$ are considered to satisfy edge support boundary conditions.

The velocity potential Φ satisfies the partial differential equation

$$\nabla^2_{xyz}\Phi_j = 0 \text{ at } -\infty < x, z < \infty, 0 < y < h \tag{A1}$$

The linearised free surface boundary condition, dynamic free surface boundary condition and bottom boundary condition are the same as in Eqs. (2–4). The plate-covered boundary condition based on the Timoshenko-Mindlin plate theory (Magrab 1979) for $-a<x<0, -\infty<z<\infty$, is given by

$$\left\{\left(EI\nabla^2_{xz}-m_sI\partial_t^2\right)\left(\nabla^2_{xz}-\frac{m_sS}{EI}\partial_t^2\right)+m_s\partial_t^2\right\}\Phi_{2y} + \rho g\left(1-S\nabla^2_{xz}+\frac{m_sIS}{EI}\partial_t^2\right)\Phi_{2y} = \rho\left(1-S\nabla^2_{xz}+\frac{m_sIS}{EI}\partial_t^2\right)\partial_t^2\Phi_2 \tag{A2}$$

where ρ is the density of water, m_s is the mass of the plate, $I=d^2/12$ is the rotary inertia and $S=EI/\mu Gd$ is the shear deformation for the Timoshenko-Mindlin equation. The structural edge conditions for oblique wave interaction with floating thick elastic plate are as follows:

Case I: freely floating elastic plate

The freely floating elastic plate represents zero bending moment and zero shear force at the plate edge. In the case of finite water depth, the shear force and bending moment at the plate edge $x=0$ and $x=-a$ satisfy the relation given by

$$EI\left(\frac{\partial}{\partial x^2}+\nu\frac{\partial}{\partial z^2}\right)\partial_y\Phi_2 = 0 \text{ and } \left[EI\frac{\partial}{\partial x}\left\{\nabla^2_{xz}+(1-\nu)\frac{\partial}{\partial z^2}\right\}+m_s\omega^2(S+I)\right]\partial_y\Phi_2 = 0 \tag{A3}$$

Case II: simply supported floating elastic plate

In this case, the simply supported edge condition represents the bending moment and deflection to vanish at the edges or at the supports for finite water depth. The plate edge is considered to be having zero deflection and zero bending moment at $x=0,-a$ satisfying the relation

$$\partial_y\Phi_2 = 0 \quad \text{and} \quad EI\left(\frac{\partial}{\partial x^2}+\nu\frac{\partial}{\partial z^2}\right)\partial_y\Phi_2 = 0 \tag{A4}$$

Case III: fixed edge floating elastic plate

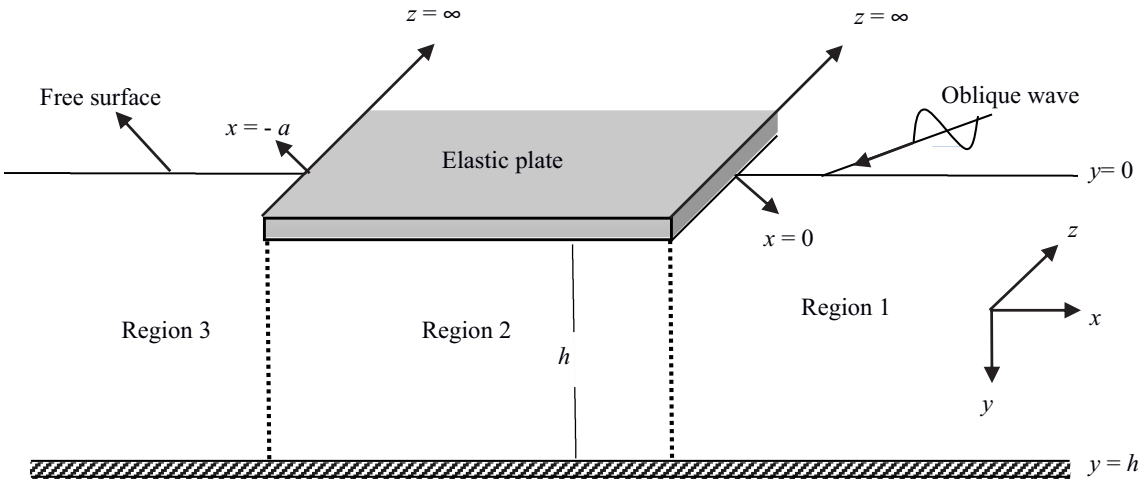

Fig. A1 Schematic diagram for floating elastic plate under oblique wave incidence

In this case of fixed edge condition, the deflection and slope vanish at the support. In finite water depth, we consider zero deflection and zero slope at the plate edge $x = 0, -a$ which satisfy the relation

$$\partial_y \Phi_2 = 0 \text{ and } \partial_{xy}^2 \Phi_2 = 0 \text{ at } y = 0 \tag{A5}$$

Assuming that the wave elevation and the plate deflection are simple harmonic motion in time with the frequency ω, the velocity potential $\Phi_j(x, y, z, t)$ and the surface deflection $\zeta_j(x, z, t)$ can be written as $\Phi_j(x, y, z, t) = \text{Re}\{\phi_j(x, y)e^{ilz - i\omega t}\}$ and $\zeta_j(x, z, t) = \text{Re}\{\zeta_j(x)e^{ilz - i\omega t}\}$ where Re denotes the real part, and l is the component of the wave number along the z-direction which is of the form $l = \gamma_{10} \sin\theta$. Thus, the spatial velocity potential $\phi_j(x, y)$ satisfies Helmholtz's equation. The continuity of velocity and pressure at the interface $x = -a$ and $x = 0$ for $j = 1, 2$; $0 < y < h$, and the velocity potential in each of the open water and plate-covered region are the same as described in Sections 2 and 3 where the eigenfunctions $f_{jn}(y)$'s are given by

$$f_{jn}(y) = \frac{\cosh \gamma_{jn}(h-y)}{\cosh \gamma_{jn} h} \text{ for } n = 0, \text{I}, \text{II} \text{ and } f_{jn}(y)$$
$$= \frac{\cos \gamma_{jn}(h-y)}{\cos \gamma_{jn} h} \text{ for } n = 1, 2, \ldots \tag{A6}$$

where γ_{jn} for $j = 1, 3$ and $n = 0$ are the eigenvalues that satisfy the dispersion relation in the open water region given by

$$\gamma_{j0} \tanh \gamma_{j0} h - \omega^2/g = 0 \tag{A7}$$

with $\gamma_{jn}^2 = k_{jn}^2 + l^2$ where $l = \gamma_{10} \sin\theta$. In addition, there are an infinite number of purely imaginary roots $\gamma_{jn} = i\gamma_{jn}$ for $n = 1, 2....$ with $\gamma_{jn}^2 = k_{jn}^2 - l^2$. In the plate-covered region, the eigenvalues γ_{jn} for $j = 2$ satisfy the dispersion relation given by

$$\left(\alpha_0 - \alpha_1 \gamma_{jn}^2 + \alpha_2 \gamma_{jn}^4\right) \gamma_{jn} \tanh \gamma_{jn} h - \left(\beta_0 - \beta_1 \gamma_{jn}^2\right) = 0 \tag{A8}$$

where α_0, α_1, α_2, β_0, and β_1 are the same as defined in Eq. (20). Proceeding in a similar manner as in Section 4, applying the mode-coupling relation along with using the continuity of mass flux and pressure across the interfaces as in Eq. (8) and the edge support conditions, a system of linear equations can be obtained for the determination of the unknown coefficients whose details are deferred here to avoid repetition.

References

Andrianov AI, Hermans AJ (2003) The influence of water depth on the hydroelastic response of a very large floating platform. Mar Struct 16(5):355–371. https://doi.org/10.1016/S0951-8339(03)00023-6

Andrianov AI, Hermans AJ (2006) Hydroelastic analysis of floating plate of finite draft. Appl Ocean Res 28:313–325. https://doi.org/10.1016/j.apor.2006.12.002

Balmforth NJ, Craster RV (1999) Ocean waves and ice sheets. J Fluid Mech 395:89–124. https://doi.org/10.1017/S0022112099005145

Chen XJ, Wu YS, Cui WC, Jensen JJ (2006) Review of hydroelasticity theories for global response of marine structures. Ocean Eng 33(3–4):439–457. https://doi.org/10.1016/j.oceaneng.2004.04.010

Fox C, Squire VA (1991) Coupling between the ocean and an ice shelf. Ann Glaciol 15:101–108. https://doi.org/10.3189/1991AoG15-1-101-108

Gao RP, Tay ZY, Wang CM, Koh CG (2011) Hydroelastic response of very large floating structure with a flexible line connection. Ocean Eng 38:1957–1966. https://doi.org/10.1016/j.oceaneng.2011.09.021

Gao RP, Wang CM, Koh CG (2013) Reducing hydroelastic response of pontoon-type very large floating structures using flexible connector and gill cells. Eng Struct 52:372–383. https://doi.org/10.1016/j.engstruct.2013.03.002

Guo Y, Liu Y, Meng X (2016) Oblique wave scattering by a semi-infinite elastic plate with finite draft floating on a step topography. Acta Oceanol Sin 35(7):113–121. https://doi.org/10.1007/s13131-015-0760-2

Hermans AJ (2003) Interaction of free surface waves with a floating dock. J Eng Math 45:39–53. https://doi.org/10.1023/A:1022042120610

Hermans AJ (2004) Interaction of free-surface waves with floating flexible strips. J Eng Math 49(2):133–147. https://doi.org/10.1023/B:ENGI.0000017477.58851.af

Hermans AJ (2007) Free-surface wave interaction with a thick flexible dock or very large floating platform. J Eng Math 58(1–4):77–90. https://doi.org/10.1007/s10665-006-9104-8

Karmakar D, Guedes Soares C (2012) Scattering of gravity waves by a moored finite floating elastic plate. Appl Ocean Res 34:135–149. https://doi.org/10.1016/j.apor.2011.09.002

Karmakar D, Sahoo T (2006) In: Dandapat BS, Majumder BS (eds) Flexural gravity wavemaker problem-revisited, *International Conference on Application of Fluid Mechanics in Industry and Environment, ISI, Kolkata, India,* Fluid mechanics in industry and environment. Research Publishing Services, Singapore, 285–291 http://rpsonline.com.sg/rpsweb/icafmie.html

Karmakar D, Bhattacharjee J, Sahoo T (2007) Expansion formulae for wave structure interaction problems with applications in hydroelasticity. Int J Eng Sci 45:807–828. https://doi.org/10.1016/j.ijengsci.2007.06.002

Karmakar D, Bhattacharjee J, Sahoo T (2009) Wave interaction with multiple articulated floating elastic plates. J Fluids Struct 25(6):1065–1078. https://doi.org/10.1016/j.jfluidstructs.2009.03.005

Karperaki AE, Belibassakis KA, Papathanasiou TK (2016) Time-domain, shallow-water hydroelastic analysis of VLFS elastically connected to the seabed. Mar Struct 48:33–51. https://doi.org/10.1016/j.marstruc.2016.04.002

Kashiwagi M (2000) Research on hydroelastic responses of VLFS: recent progress and future work. Int J Offshore Polar Eng 10(2):81–90 http://legacy.isope.org/publications/journals/ijope-10-2/abst-10-2-p081-WK-45-Kashiwagi.pdf

Khabakhpasheva TI, Korobkin AA (2002) Hydroelastic behaviour of compound floating plate in waves. J Eng Math 44(1):21–40. https://doi.org/10.1023/A:1020592414338

Kohout AL, Meylan MH (2009) Wave scattering by multiple floating elastic plates with spring or hinged boundary conditions. Mar Struct 22(4):712–729. https://doi.org/10.1016/j.marstruc.2009.06.005

Koley S, Mondal R, Sahoo T (2018) Fredholm integral equation technique for hydroelastic analysis of a floating flexible porous plate. Eur J Mech / B Fluids 67:291–305. https://doi.org/10.1016/j.euromechflu.2017.10.004

Loukogeorgaki E, Yagci O, Kabdasli MS (2014) 3D experimental investigation of the structural response and the effectiveness of a moored floating breakwater with flexibly connected modules. Coast Eng 91:164–180. https://doi.org/10.1016/j.coastaleng.2014.05.008

Loukogeorgaki E, Lentsiou EN, Aksel M, Yagci O (2017) Experimental investigation of the hydroelastic and the structural response of a moored pontoon-type modular floating breakwater with flexible connectors. Coast Eng 121:240–254. https://doi.org/10.1016/j.coastaleng.2016.09.002

Magrab EB (1979) Vibration of elastic structural members. Springer Netherlands, Springer Science & Business Media B.V https://www.springer.com/gp/book/9789028602076

Manam SR, Bhattacharjee J, Sahoo T (2006) Expansion formulae in wave structure interaction problems. Proc Roy Soc London A 462(2065):263–287

Meylan MH, Squire VA (1994) The response of ice floes to ocean waves. J Geophys 99:891–900. https://doi.org/10.1029/93JC02695

Meylan MH, Squire VA (1996) Response of a circular ice-floe to ocean waves. J Geophys Res 101:8869–8884. https://doi.org/10.1029/95JC03706

Mindlin RD (1951) Influence of rotary inertia and shear on flexural motion of isotropic elastic plates. J Appl Mech (ASME) 18:31–38 http://appliedmechanics.asmedigitalcollection.asme.org/journal.aspx

Namba Y, Ohkusu M (1999) Hydroelastic behavior of floating artificial islands in waves. Int J Offshore Polar Eng 9(1):39–47 http://legacy.isope.org/publications/journals/ijope-9-1/abst-9-1-p39-WK-43-Namba.pdf

Ohkusu M, Namba Y (2004) Hydroelastic analysis of a large floating structure. J Fluids Struct 19:543–555. https://doi.org/10.1016/j.jfluidstructs.2004.02.002

Ohmatsu S (2005) Overview: research on wave loading and responses of VLFS. Mar Struct 18(2):149–168. https://doi.org/10.1016/j.marstruc.2005.07.004

Pardo ML, Iglesias G, Carral L (2015) A review of very large floating structures (VLFS) for coastal and offshore uses. Ocean Eng 109:677–690. https://doi.org/10.1016/j.oceaneng.2015.09.012

Praveen KM, Karmakar D, Nasar T (2016) Hydroelastic analysis of floating elastic thick plate in shallow water depth. Perspect Sci 8:770–772. https://doi.org/10.1016/j.pisc.2016.06.084

Praveen KM, Karmakar D, Guedes Soares C (2018) Hydroelastic analysis of articulated floating elastic plate based on Timoshenko-Mindlin's theory. Ships Offshore Struct 13(S1):287–301. https://doi.org/10.1080/17445302.2018.1457236

Rao SS (2007) Vibration of continuous systems. John Wileys, Hoboken. https://doi.org/10.1002/9780470117866

Sahoo T, Yip TL, Chwang AT (2001) Scattering of surface waves by a semi-infinite floating elastic plate. Phys Fluids 13(11):3215–3222. https://doi.org/10.1063/1.1408294

Tay ZY, Wang CM (2012) Reducing hydroelastic response of very large floating structures by altering their plan shapes. Ocean Systems Engineering 2:69–81. https://doi.org/10.12989/ose.2012.2.1.069

Taylor RE, Ohkusu M (2000) Green functions for hydroelastic analysis of vibrating free-free beams and plates. Appl Ocean Res 22(5):295–314. https://doi.org/10.1016/S0141-1187(00)00018-3

Teng B, Cheng L, Liu SX, Li FJ (2001) Modified eigenfunction expansion methods for interaction of water waves with a semi-infinite elastic plate. Appl Ocean Res 23(6):357–368. https://doi.org/10.1016/S0141-1187(02)00005-6

Timoshenko SP, Krieger SW (1959) Theory of plates and shells. McGraw-hill, New York https://www.mheducation.com/

Wang S, Karmakar D, Guedes Soares C (2016) Hydroelastic impact of a horizontal floating plate with forward speed. J Fluids Struct 60:97–113. https://doi.org/10.1016/j.jfluidstructs.2015.11.005

Watanabe E, Utsunomiya T, Wang CM (2004) Hydroelastic analysis of pontoon-type VLFS: a literature survey. Eng Struct 26:245–256. https://doi.org/10.1016/j.engstruct.2003.10.001

Williams TD, Bennetts LG, Squire VA, Dumont D, Bertino L (2013) Wave-ice interactions in the marginal ice zone. Part 1: theoretical foundations. Ocean Model 71:81–91. https://doi.org/10.1016/j.ocemod.2013.05.010

Xu F, Lu DQ (2009) An optimization of eigenfunction expansion method for the interaction of water waves with an elastic plate. J Hydrodyn 21(4):526–530. https://doi.org/10.1016/S1001-6058(08)60180-8

Xu F, Lu DQ (2011) Hydroelastic interaction between water waves and a thin elastic plate of arbitrary geometry. Sci China: Phys Mech Astron 54(1):59–66. https://doi.org/10.1007/s11433-010-4199-3

Zhao C, Hao X, Liang R, Lu J (2015) Influence of hinged conditions on the hydroelastic response of compound floating structures. Ocean Eng 101:12–24. https://doi.org/10.1016/j.oceaneng.2015.04.021